ASC Coordinates: Rev 3.0 Draft

Jonathan McDowell

April 26, 1996

Contents

List of Tables

List of Figures

1 General Introduction

There are a lot of different coordinate systems used in the AXAF program, mostly intended for use in constructing and aligning the hardware. This memo is intended to give the ASC SDS group's current understanding of the relationships between them (Gratings and mirror metrology systems are not yet included) and to define many more systems, which are useful for data analysis of observations both in flight and at XRCF.

1.1 Notational conventions

1.1.1 Pixel convention

In all cases where we use discrete **pixel numbers**, the corresponding **pixel coordinates** are defined to be equal to the pixel number at the center of the pixel. We further recommend that for finite detector planes, the lower left pixel be numbered (1,1) so that its center has coordinates (1.0, 1.0). If the detector is rectangular with sides of length XMAX, YMAX the pixel coordinates then run from (0.5, 0.5) in the lower left corner (LL) to (XMAX+0.5, YMAX+0.5) in the upper right corner (UR) while the pixel numbers in each axis run from 1 to XMAX, 1 to YMAX.

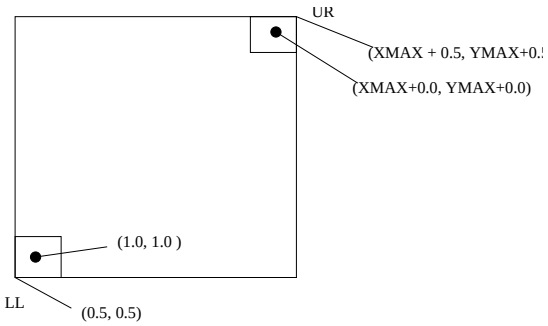

Figure 1: Pixel convention.

1.1.2 Vector and coordinate notation

A bold face symbol e.g. $\boldsymbol{B}$ denotes a point in 3D space. The notation $Y_A(\boldsymbol{B})$ denotes the Y coordinate of point $\boldsymbol{B}$ in the 3-dimensional Cartesian coordinate system A. When we refer to a point as an argument in this way we usually get lazy and omit the boldface, e.g. $Y_A(B)$. The notation $P_A(B)$ denotes the triple $(X_A(B), Y_A(B), Z_A(B))$, i.e. the coordinates of $\boldsymbol{B}$ in the A coordinate system. (P is not in boldface since it is not a vector - it is in a specific coordinate system.)

1.1.3 Rotation and translation of Cartesian systems

The general transformation from a cartesian system A to a system B involves a scaling, a translation, and a rotation. This may be described by seven numbers: the scale factor K_{AB} (choice of units), the position vector $P_B(A0) = (X_B(A0), Y_B(A0), Z_B(A0))$ of the origin of A in the B system, and the three Euler angles ϕ_E, θ_E, ψ_E of the rotation R(A,B) from A to B, (see Appendix 1),

$$\begin{aligned} R(A,B) &= Rot(\phi_E, \theta_E, \psi_E) \\ &= \begin{pmatrix} \cos\phi_E \cos\theta_E \cos\psi_E - \sin\phi_E \sin\psi_E & \sin\phi_E \cos\theta_E \cos\psi_E + \cos\phi_E \sin\psi_E & -\sin\theta_E \cos\psi_E \\ -\cos\phi_E \cos\theta_E \sin\psi_E - \sin\phi_E \cos\psi_E & -\sin\phi_E \cos\theta_E \sin\psi_E + \cos\phi_E \cos\psi_E & \sin\theta_E \sin\psi_E \\ \cos\phi_E \sin\theta_E & \sin\phi_E \sin\theta_E & \cos\theta_E \end{pmatrix} \end{aligned} \tag{1}$$

Then coordinates of a general point G

$$P_A(G) = (X_A(G), Y_A(G), Z_A(G)) \tag{2}$$

may be converted to

$$P_B(G) = (X_B(G), Y_B(G), Z_B(G)) \tag{3}$$

using the formula

$$\boxed{P_B(G) = R(A,B) K_{AB} P_A(G) + P_B(A0)} \tag{4}$$

If

$$R(A,B) = Rot(\phi_E, \theta_E, \psi_E) \tag{5}$$

then

$$R(B,A) = Rot(\pi - \psi_E, \theta_E, \pi - \phi_E). \tag{6}$$

Further, if C is related to B by reflection about the X axis, i.e. $Y_C = -Y_B, Z_C = -Z_B$ then

$$R(A,C) = Rot(\phi_E, \pi + \theta_E, \pi - \psi_E). \tag{7}$$

1.1.4 Spherical polar coordinates

We also use spherical polar coordinate systems. The WCS paradigm describes general rotations of a spherical polar coordinate system. We define the native cartesian axes X,Y,Z of a spherical polar system (r, θ, ϕ) by the equation

$$(X, Y, Z) = r\mathcal{S}(\theta, \phi) = (r\cos\phi\sin\theta, r\sin\phi\sin\theta, r\cos\theta) \tag{8}$$

so that the north pole is through the positive Z axis and the azimuth is zero along the positive X axis and 90 degrees along the positive Y axis. Any other choice of spherical coordinates (r, θ', ϕ') may be defined by specifying the Euler rotation matrix which rotates the corresponding native systems into each other. In the appendix I derive

$$\boxed{\begin{aligned} \theta' &= \cos^{-1}\left(\cos\theta_E \cos\theta + \sin\theta_E \sin\theta \cos(\phi - \phi_E)\right) \\ \phi' &= \arg\left(\cos\theta_E \sin\theta \cos(\phi - \phi_E) - \sin\theta_E \cos\theta, \sin\theta \sin(\phi - \phi_E)\right) - \psi_E \end{aligned}} \tag{9}$$

1.2 AXAF overview

1.2.1 AXAF Reference Points

There are several crucial reference points we use:

- $\boldsymbol{H1}$, the HRMA CAP (Central Aperture Plate) reference point. This is the fundamental positional alignment reference and the origin of HRMA coordinates.
- $\boldsymbol{H0}$, the HRMA nodal point. This is the fundamental data analysis positional reference, although its location in spacecraft coordinates is a derived quantity. It plays two roles: firstly, it is the nominal 'thin lens' position from which we measure off-axis angles at the focal plane - it's where the photons 'appear to come from'. If this were exactly true, we'd have a constant plate scale, but actually the effective nodal point depends both on energy and off-axis angle. Nevertheless, we can adopt a conventional nodal point and make astrometric position corrections as a function of position and energy, relative to the positions derived using that conventional nodal point.
- $\boldsymbol{G0}$, the Grating nodal point.
- $\boldsymbol{G1}$, the origin of OTG coordinates.
- $\boldsymbol{X0}$, the XRCF coordinate origin which coincides with $\boldsymbol{H1}$, the HRMA CAP reference point when HRMA is in its XRCF default position.
- $\boldsymbol{X1}$, the AXAF spacecraft coordinate origin which is a fictitious point out in space behind the SIM.
- $\boldsymbol{F}$, the HRMA focus (or XSS conjugate focus, at XRCF).
- $\boldsymbol{F0}$, the point in the XRCF where the HRMA focus lies when the HRMA is at its default position.
- $\boldsymbol{\Sigma_0}$, the SIM reference point, which is identical with the HRMA focus $\boldsymbol{F}$ when the SIM is installed in flight.
- $\boldsymbol{S}$, the nominal focus position on one of the four detectors ACIS-I, ACIS-S, HRC-I, HRC-S.
- $\boldsymbol{\Sigma}$, the reference point on the SIM transfer table.
- $\boldsymbol{A0}$, the center of the aperture in the spacecraft-to-IUS interface plane.
- $\boldsymbol{A1}$, the center of the aperture at the front edge of the paraboloids (which is the origin of the ray trace system).
- $\boldsymbol{LL}$, the origin ('lower left corner', *sic*) of one of the 14 chips making up one of the 4 detectors on the 2 instruments.

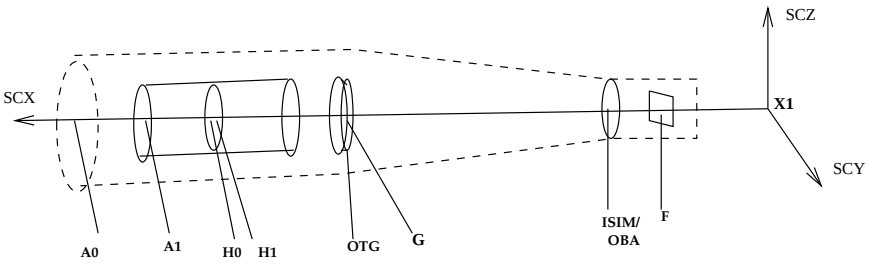

Figure 2: Schematic of interesting points in the spacecraft

1.2.2 Spacecraft coordinates (SC-1.0)

The Spacecraft (Observatory) coordinate system X_A, Y_A, Z_A (SC/TS ICD 4 Nov 1992, 3.2.1.1.1) is as follows: [1],[2] The X axis is parallel to the HRMA centerline; the aperture is toward positive X, while the SIM is at lower values of X. The Y and Z axes are in the plane of the SIM, such that the ACIS radiator is toward positive Z and the Y axes completes an X, Y, Z right handed set. The coordinates are also called SCX, SCY, SCZ when we want to refer to a spacecraft coordinate system in general rather than AXAF in particular. (X_A, Y_A, Z_A) are measured in 'inches', which is a unit of length defined to be exactly 0.02540m. The center of the aperture in the AXAF/IUS interface plane is defined to have coordinates (500, 0, 0). The spacecraft trunnion plane has SCZ=14. The coordinates of the HRMA nodal point ***H0*** in SC coordinates are $(X_A(H0), 0, 0)$ where the value of $X_A(H0)$ is 428.116. The focus is at $(31.836, 0.0, 0.0)$.

1.2.3 HRMA coordinates (HRMA-2.0)

The project has defined Cartesian coordinates (X_H, Y_H, Z_H) fixed in the HRMA cap midplane, which are called **HRMA coordinates**. The origin of HRMA coordinates ***H1*** is at the HRMA CAP reference point. The HRMA X_H axis is along the HRMA optical axis, and positive X is toward the entrance aperture. Units of HRMA coordinates shall be mm.

1.2.4 HRMA nodal coordinates (HNC, HRMA-1.1)

The Spacecraft and HRMA coordinate systems are the fundamental ones for hardware alignment, but for data analysis of observations it's easier to use the HRMA nodal point ***H0*** as origin. This point is calculated to be offset by 17.577 mm from the HRMA CAP midplane (the value may change). The HRMA nodal coordinate (HNC) system is (X_N, Y_N, Z_N), where

$$\begin{pmatrix} X_N \\ Y_N \\ Z_N \end{pmatrix} = \begin{pmatrix} X_H - X_H(H0) \\ Y_H \\ Z_H \end{pmatrix} \tag{10}$$

where $X_H(H0) = -17.577$. The finite conjugate focus is at HRMA nodal coordinates (-10258.3, 0.0, 0.0). (IF1-20 Obs/SI ICD). Note that

$$\begin{pmatrix} X_N \\ Y_N \\ Z_N \end{pmatrix} = \begin{pmatrix} (SCX - SCX(H0)) * 25.4 \\ SCY * 25.4 \\ SCZ * 25.4 \end{pmatrix} \tag{11}$$

where SCX(H0) (or $X_A(H0)$) is +428.116.

In the following table are listed reference points for various parts of the spacecraft. For XRCF, I give XRCF coordinates in inches for easy comparison with the drawings, although elsewhere in this document XRCF coordinates are measured in mm.

Table 1: Interesting points in spacecraft and HRMA nodal coordinates

Flight				
Point	Description	(X_A, Y_A, Z_A)	(X_N, Y_N, Z_N)	Ref
X1	SC coordinate origin	(0.0, 0.0, 0.0)	(-10874.146, 0.0, 0.0)	
F	Flight Focus	(31.836, 0.0, 0.0)	(-10065.500, 0.0, 0.0)	[1],p.9
	Translation Table surface	(55.836, 0.0, 0.0)	(-9455.91, 0.0, 0.0)	[1],p.17
	ISIM to OBA interface	(60.336, 0.0, 0.0)	(-9341.6, 0.0, 0.0)	[1],p.9
G1	OTG Origin	(369.245, 0.0, 0.0)	(-1495.3, 0.0, 0.0)	[1],dr. 301331/3
	OTG Datum	(370.915, 0.0, 0.0)	(-1452.9, 0.0, 0.0)	[1],dr. 301331/3
G0	OTG Node	(371.745, 0.0, 0.0)	(-1431.810, 0.0, 0.0)	[1], dr.301331/3
H1	HRMA CAP reference point	(427.745, 0.0, 0.0)	(-9.42, 0.0, 0.0)	[1], dr.301331/3
H0	HRMA nodal point	(428.116, 0.0, 0.0)	(0.0, 0.0, 0.0)	[1], dr.30133/31
A1	Front end of paraboloids	(462.474, 0.0, 0.0)	(872.692, 0.0, 0.0)	
A0	Aperture center in IUS I/F plane	(500.0, 0.0, 0.0)	(1825.85, 0.0, 0.0)	[2],[1],p.9

XRCF				
Point	Description	X_{XRCF} (in)	(X_N, Y_N, Z_N)	Ref
F0	XRCF Default Focus	-403.5	(-10258.3, 0.0, 0.0)	[1], dr. 301331/5
G1	OTG Origin at XRCF	-60.613	(-1549.0, 0.0, 0.0)	[1]
	OTG Datum at XRCF	-58.943	(-1506.57, 0.0, 0.0)	[1]
G0	OTG Node at XRCF	-58.113	(-1485.49, 0.0, 0.0)	[1]
H1	HRMA CAP reference point	0.0	(-9.42, 0.0, 0.0)	
H0	HRMA nodal point	-0.37	(0.0, 0.0, 0.0)	

1.2.5 Identification convention

For each coordinate system definition used in data analysis, we give an identifier which encodes both the purpose of the coordinate system and a version number for the coordinate system. As we revise definitions of the coordinate systems, the version numbers will be changed. The identifiers will be present in ASC-generated data files so that the coordinates used in data can be unambiguously determined. (In FITS files, I suggest the use of an ACSYSn keyword to hold the identifiers). For instance, if the defining constants of ACIS tiled detector coordinates are altered, the new system will be labelled ACIS-2.1 instead of ACIS-2.0. There was error in the description of the definition of HSC-1.0 (rev 2.2 of this document and earlier) and so the corrected, consistent definition is identified as HSC-1.1. Note that a single coordinate system definition (and identifier) may actually refer to more than one coordinate system, e.g. AXAF-CPC-1.0 defines a coordinate system on each of the 14 different detector chips separately.

The fundamental coordinate system in flight is the AXAF-SC-1.0 system (spacecraft coordinates), but for data analysis both in flight and at XRCF our primary coordinate system will be the HRMA-1.1 nodal coordinate system, defined to be fixed in the HRMA mirror. At XRCF, another fundamental system is the XRCF-1.0 system.

The pixel coordinate systems also have generic identifiers, since some derived data files may hold both ACIS and HRC (and ROSAT?!) pixel values in the same columns.

Table 2: Coordinate System Catalog

Identifier	Name of system	Notation	Type	Origin	Status/Use
AXAF-ACIS-1.0	ACIS chip	CHIPX, CHIPY	Pixel (CHIP)	$\boldsymbol{LL}$	Primary
AXAF-ACIS-2.0	ACIS detector	DETX, DETY	Pixel (DET)		Deleted (Rev 2.3)
AXAF-ACIS-2.2	ACIS detector	DETX, DETY	Pixel (DET)		Primary
AXAF-ACIS-2.3	ACIS detector	DETX, DETY	Pixel (DET)		Alternative
AXAF-ACIS-2.3A	ACIS detector	DETX, DETY	Pixel (DET)		Alternative (XRCI
AXAF-ACIS-3.0	ACIS readout	RAWX,RAWY	Pixel (RAW)	$\boldsymbol{LL}$	Reference
AXAF-CHIP-1.0	Chip	CHIPX, CHIPY	Pixel (CHIP)		Generic
AXAF-CPC-1.0	Chip physical	$(X_{CPC}, Y_{CPC}, Z_{CPC})$	3D	$\boldsymbol{H0}$	Analysis
AXAF-DET-2.0	Tiled detector	DETX, DETY	Pixel (DET)		Generic
AXAF-DFC-1.0	Default FAM	$(X_{DFC}, Y_{DFC}, Z_{DFC})$	3D	$\boldsymbol{F0}$	Primary (XRCF)
AXAF-FAM-1.0	FAM	$(X_{FAM}, Y_{FAM}, Z_{FAM})$	3D	$\boldsymbol{\Sigma_0}$	Analysis (XRCF)
AXAF-FP-1.0	Focal Plane Pixel	FPX, FPY	Pixel		Analysis
AXAF-FP-2.0	Dithered Focal Plane	DFPX, DFPY	Pixel		Alternative
AXAF-GDC-1.0	Grating Diffraction	r_{TG}, d_{TG}		$\boldsymbol{ZO}$	Primary?
AXAF-GDP-1.0	Grating Diffraction Plane Pixel	GDX,GDY	Pixel		Primary
AXAF-GZO-1.0	Grating Zero Order	$(X_{GZO}, Y_{GZO}, Z_{GZO})$	3D	$\boldsymbol{G0}$	Analysis
AXAF-HRC-1.0	HRC chip	CHIPX, CHIPY	Pixel (CHIP)	$\boldsymbol{LL}$	Deleted (Rev 2.3)

AXAF-HRC-1.1	HRC chip	CHIPX, CHIPY	Pixel (CHIP)	$\boldsymbol{LL}$	Primary
AXAF-HRC-2.0I	HRC-I detector	DETX, DETY	Pixel (DET)		Deleted (Rev 2.3)
AXAF-HRC-2.0S	HRC-S detector	DETX, DETY	Pixel (DET)		Deleted (Rev 2.3)
AXAF-HRC-2.1S	HRC-S detector	DETX, DETY	Pixel (DET)		Deleted (Rev 2.3)
AXAF-HRC-2.2I	HRC-I detector	DETX, DETY	Pixel (DET)		Primary
AXAF-HRC-2.2S	HRC-S detector	DETX, DETY	Pixel (DET)		Primary
AXAF-HRC-2.3I	HRC-I detector	DETX, DETY	Pixel (DET)		Alternative
AXAF-HRC-2.3S	HRC-S detector	DETX, DETY	Pixel (DET)		Alternative
AXAF-HRC-3.0	HRC raw pixel	RAWX, RAWY	Pixel (RAW)	$\boldsymbol{LL}$	Alternative
AXAF-HRC-4.0	HRC telemetry	u_{HT}, v_{HT}	Pixel (RAW)	-	Analysis
AXAF-HRC-5.0	HRC degap		Pixel (CHIP)	$\boldsymbol{LL}$	Deleted
AXAF-HRC-6.0	HRC tap	u, v	Pixel (CHIP)	$\boldsymbol{LL}$	Analysis
AXAF-HRMA-1.0	XRCF mirror	(X_M, Y_M, Z_M)	3D	$\boldsymbol{H0}$	Deleted (Rev 2.3)
AXAF-HRMA-1.1	HRMA nodal	(X_N, Y_N, Z_N)	3D	$\boldsymbol{H0}$	Analysis
AXAF-HRMA-2.0	HRMA	(X_H, Y_H, Z_H)	3D	$\boldsymbol{H1}$	Reference
AXAF-HRMA-3.0	SAOSAC	$(X_{SAC}, Y_{SAC}, Z_{SAC})$	3D	$\boldsymbol{A1}$	Reference
AXAF-HRMA-4.0	Project Focal Plane	(X_F, Y_F, Z_F)	3D	$\boldsymbol{F}$	Reference
AXAF-HSC-1.1	HRMA spherical	(r, θ_H, ϕ_H)	Spherical	$\boldsymbol{H0}$	World
AXAF-HSC-2.0	HRMA source	$(r, \mathrm{az}, \mathrm{el})$	Spherical	$\boldsymbol{H0}$	World
AXAF-HSC-3.0	HRMA rotation (pitch and yaw)	(r, α_z, α_y)	Spherical	$\boldsymbol{H0}$	World
AXAF-LSI-1.0	Local Science Inst.	$(X_{LSI}, Y_{LSI}, Z_{LSI})$	3D	$\boldsymbol{S}$	Deleted (Rev 2.3)
AXAF-LSI-1.1	Local Science Inst.	$(X_{LSI}, Y_{LSI}, Z_{LSI})$	3D	$\boldsymbol{S}$	Analysis
AXAF-OTG-1.0	Grating Nodal	$(X_{GNC}, Y_{GNC}, Z_{GNC})$	3D	$\boldsymbol{G0}$	Analysis
AXAF-OTG-2.0	OTG	(X_G, Y_G, Z_G)	3D	$\boldsymbol{G1}$	Reference
AXAF-PSP-1.0	Physical Sky Plane	$(X_{PSP}, Y_{PSP}, Z_{PSP})$	3D	-	Analysis
AXAF-PTP-1.0	Physical Tangent Plane	$(X_{PTP}, Y_{PTP}, Z_{PTP})$	3D	$\boldsymbol{H0}$	Analysis
AXAF-SC-1.0	Spacecraft	SCX, SCY, SCZ or (X_A, Y_A, Z_A)	3D	$\boldsymbol{X1}$	Reference
AXAF-SKY-1.0	Sky pixel	X, Y	Pixel (SKY)		Primary
AXAF-STF-1.0	SIM Travel Frame	$(X_{STF}, Y_{STF}, Z_{STF})$	3D	$\boldsymbol{\Sigma_0}$	Analysis
AXAF-STF-2.0	SIM Installation Frame	$(X_{SIC}, Y_{SIC}, Z_{SIC})$	3D	$\boldsymbol{\Sigma_0}$	Analysis (XRCF)
AXAF-STT-1.0	SIM Translation Table	$(X_{STT}, Y_{STT}, Z_{STT})$	3D	$\boldsymbol{\Sigma}$	Deleted (Rev 2.3)
AXAF-STT-1.1	SIM Translation Table	$(X_{STT}, Y_{STT}, Z_{STT})$	3D	$\boldsymbol{\Sigma}$	Analysis
AXAF-TP-1.0	Tangent Plane pixel	TPX, TPY	Pixel (TP)		Primary
AXAF-XRCF-1.0	XRCF facility	$(X_{XRCF}, Y_{XRCF}, Z_{XRCF})$		$\boldsymbol{X0}$	Analysis (XRCF)

The Status/Use column describes how the coordinate system is used in data analysis:

- Primary: one of the fundamental coordinate systems for data analysis, will be stored in standard data products.
- Analysis: Used in standard data processing, at least by implication, as an intermediate step used in deriving a primary system.
- World: Angular system applied as a world coordinate system to one of the primary systems.
- Alternative: Not required in deriving the primary systems, but may be useful in inspecting the data.
- Reference: Not expected to be used in data analysis, presented for reference only.
- Deleted: Identifier refers to an earlier definition of the coordinate system which is now considered obsolete. The revision of this document in which the system was previously defined is noted.
- Generic: indicates data which may include coordinates from different instruments. For example, ACIS and HRC detector coordinates may be lumped together as AXAF-DET-2.0 (presumably in a table with a separate column indicating which instrument is meant for each row.)

1.3 Observing configurations

In this section I summarize the basic layout, referring to some coordinate systems which will be defined fully later on.

1.3.1 Flight Configuration

In flight, the orientation of the SIM with respect to the HRMA is fixed. In the flight nominal configuration, one of the SIs has its nominal focal point at the telescope focus. However, the SIM can be moved so that the nominal focal point and the telescope focus do not coincide (general flight configuration).

1.3.2 XRCF configurations

In the XRCF, we have the HRMA mounted on two axes - it can change its yaw (azimuth) and pitch (elevation), or equivalently the polar angle and polar azimuth. The instrument (SI) is mounted on either the FAM (Five Axis Mount) or the HXDS (HRMA X-ray Detection System). In the **default configuration** C0, the HRMA axis and the SI are aligned with the FOA (Facility Optical Axis) and the SI nominal focus S is located at the actual focus F. The X-ray Source System (XSS) is fixed in the XRCF frame and lies on the positive X_{XRCF} axis (see below).

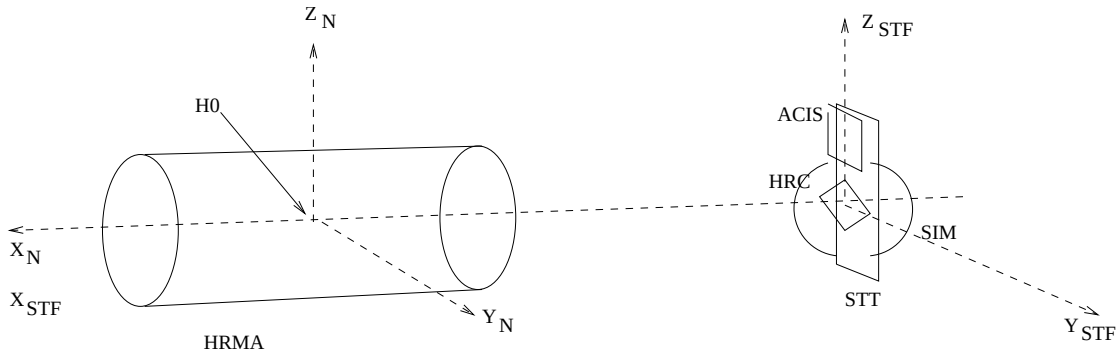

Figure 3: HRMA Nodal and STF Coordinates showing the on-orbit configuration. The SIM Transfer Table (STT) carrying the instruments moves along the Z_{STF} axis to select an instrument and along the X_{STF} axis to adjust focus.

In the **nominal configuration** CN, the HRMA is tilted but the SI is moved so that its normal X_{LSI} axis remains coincident with the HRMA optical axis X_{XRCF}. In the most general configuration the HRMA and SI are both moved relative to the XRCF but the X_{LSI} axis is not made to coincide with the X_{XRCF} axis.

WARNING: The terms '**on-axis**' and '**off-axis angle**' are correctly used to refer to an angle relative to the optical axis of the HRMA. However, at XRCF they are sometimes used to mean an angle relative to the Facility Optical Axis, which could lead to confusion. I will always use the concept of on and off axis to refer to the HRMA optical axis.

The Y_{LSI}, Z_{LSI} plane contains the science instrument, which returns coordinate values of events measured in detector pixels CHIPX, CHIPY from each of several discrete planar 'chips' (or MCPs in the case of HRC). In data analysis we consider two complementary problems:

- The forward case: Given an XRCF configuration, at which chip CHIP_ID and chip pixel CHIPX, CHIPY will the XSS photons fall? In other words, where do we expect the image to be?

- The inverse case: Given a photon landing on chip CHIP_ID and chip pixel CHIPX, CHIPY, from which direction (off-axis angle and azimuth) did the incoming photon approach the HRMA?

1.3.3 Summary of Configurations

To sum up, the range of different experimental configurations varies in complexity, with extra coordinate systems required for the more complex cases. Every time you add a new moving part, you add two new coordinate systems - one in which to describe the motion of the part and one fixed in the part to describe the positions of components relative to that part. We have:

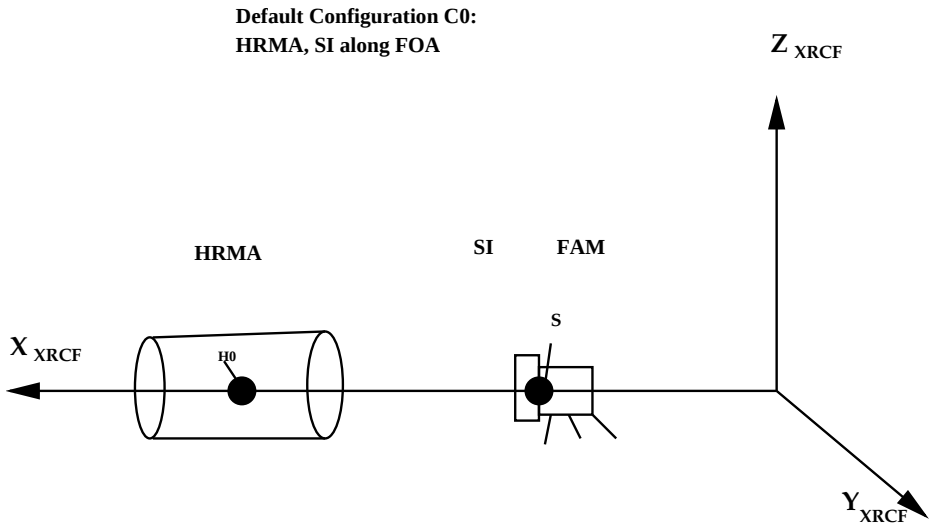

Figure 4: XRCF Coordinates showing the general configuration with HRMA, DFC and LSI coordinate systems

- XRCF default configuration, the simplest configuration with source, mirror, and SI all aligned.
- Nominal configuration (XRCF or on orbit), with the mirror and SI aligned but with the source off axis (XRCF) or with an aspect solution to be applied (on orbit). In this case we can go directly from the LSI frame to the HRMA frame without worrying about the SIM.
- SIM displaced configuration (XRCF or on orbit), with the SIM travel frame aligned with the mirror (so that the detector lies parallel to the focal plane) but with the SIM at an arbitrary position so that the telescope focus isn't at the standard place on the detector. In this case we need to deal with the SIM and SIM Travel Frame coordinate systems.
- XRCF general configuration, with the FAM moved so that the SIM travel frame is not necessarily aligned with the mirror axis. In this cases we need to use the FAM and DFC frames to link the SIM Travel frame to the HRMA frame. This gets pretty ugly!

There are three types of parameter that determine the geometrical configuration of the XRCF or the flight instrument - calibration parameters that are constant for the duration of the XRCF calibration, experiment parameters that are constant for an observation, and dynamic parameters that vary during an observation.

Table 3: Configuration parameters for XRCF observations

Calibration parameters

Table 3: Configuration parameters for XRCF observations

Quantity	Description	Best guess value XRCF
f	HRMA effective focal length	10258.3
g	Rowland Circle Diameter	
ψ_r	SI roll angle wrt HRMA in default position	0.0
$P_{XRCF}(H0)$	XRCF coordinates of HRMA nodal point	(0.0,0.0,0.0)
$\phi_{EF}, \theta_{EF}, \psi_{EF}$	Euler angles of FAM misalignment matrix R(XRCF,DFC)	(0.0,0.0,0.0)
Experiment parameters		
Quantity	Description	Default value XRCF
SI	Sub-instrument in focal plane	ACIS-S
$P_{STT}(S)$	STT coordinates of SI nominal focus	(0.0,0.0,190.5)
$P_{STF}(\Sigma)$	STF coordinates of SIM reference point	$-P_{STT}(S)$
$\theta_H(XSS)$	HRMA Polar off axis angle	0.0
$\phi_H(XSS)$	HRMA Polar azimuth	0.0
ζ_{fp}	FAM Initial polar off axis angle	$\theta_H(XSS)$

Table 3: Configuration parameters for XRCF observations

ζ_{fa}	FAM Initial polar azimuth	$\phi_H(XSS)$
df	Defocus	0.0
Dither_Pattern	Dither pattern file	None
Dither_Points	Number of dwell points	0
Dither_Dwell	Dwell time (s)	0.0
Time dependent parameters		
Quantity	Description	Default value XRCF
$P_{DFC}(FAM)$	DFC Coords of FAM, XYZ from FAM data	(0.0,0.0,0.0)
$\theta_X, \theta_Y, \theta_Z$	DFC orientation of FAM, from FAM data	(0.0,0.0,0.0)

Table 4: Configuration parameters for flight observations

Calibration parameters		
Quantity	Description	Best guess value Flight
f	HRMA effective focal length	10065.5
g	Rowland Circle Diameter	8633.69

ψ_r	SI roll angle wrt HRMA in default position	0.0
Experiment parameters		
Quantity	Description	Default value Flight
SI	Sub-instrument in focal plane	ACIS-S (at launch)
$P_{STT}(S)$	STT coordinates of SI nominal focus	(0.0,0.0,190.5)
$P_{STF}(\Sigma)$	STF coordinates of SIM reference point	$-P_{STT}(S)$
α_0, δ_0	Nominal pointing direction, J2000	No default
r_0	Nominal spacecraft roll angle	0.0
df	Defocus	0.0
Time dependent parameters		
Quantity	Description	Default value Flight
A_α, A_δ	Aspect RA and Dec offsets	0.0, 0.0
A_r	Aspect roll offset	0.0

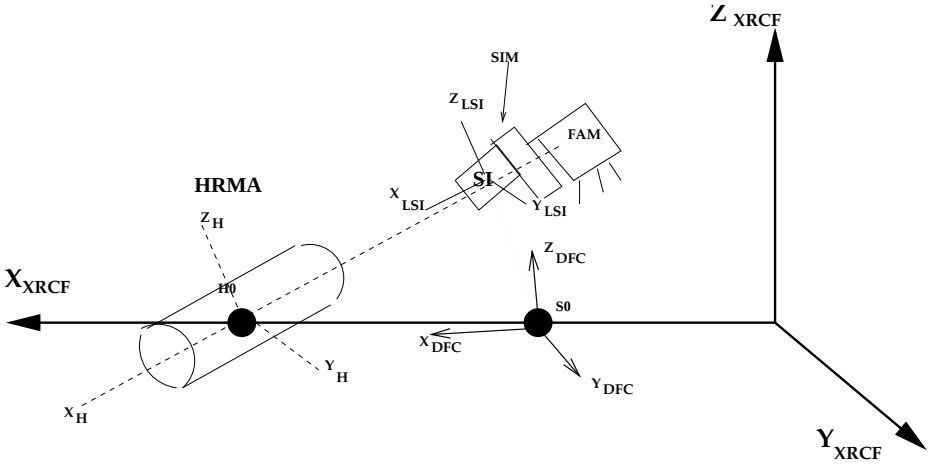

Figure 5: XRCF Coordinates showing the general configuration with HRMA and LSI coordinate systems

1.4 Data Analysis coordinate thread

In the accompanying figure, the data analysis coordinate thread is summarized. This section gives an overview of the coordinate calculation process; later sections go through each system in detail.

We start off with CHIP pixel coordinates for each planar rectangular surface that intercepts photons. The size of the CHIP pixels depends on the detector. Associated with CHIP pixel coordinates are a 'world' coordinate system in mm, called CPC (Chip Physical Coordinates). We wish to determine the direction in which the photon apparently emerged from the HRMA node in order to hit the detector surface at that pixel; this direction is expressed in HRMA Spherical Coordinates (HSC) as an off-axis angle and an azimuth. We store the HSC values as another world coordinate system attached to a two-dimensional pixel plane, the Focal Plane Pixel Coordinates (FP). The FP pixel size is not neccessarily the same as the CHIP pixel size. FP pixels are centered on the HRMA optical axis.

To get from CHIP to FP pixels (or equivalently, from CPC to HSC coordinates), we need to go through several other three-dimensional intermediate coordinate systems: LSI coordinates, which locate the chips relative to the nominal detector aimpoint; STT coordinates, which give locations relative to the origin of the SIM translation table; STF coordinates, which give locations relative to the aperture center of the fixed SIM structure; and HNC coordinates, which give locations relative to the HRMA node.

After we have the FP pixels, we need to derive TP (Tangent Plane) pixels, which have as their world coordinate system the HRMA Spherical Coordinates of the photon as it approaches the mirror from the source. The only differences between FP and TP coordinates are small corrections to account for the mirror optics, since the HRMA has a magnification of unity on-axis. These corrections are not yet known, and in prototyping I have taken them to be zero.

The TP coordinates tell us where the the incoming photon was relative to the spacecraft structure, but we want to know an absolute location on the sky. We apply the time-resolved aspect solution to TP coordinates to obtain Sky pixel coordinates, which are centered on a nominal celestial location and which have celestial angular coordinate systems such as RA and Dec as their world coordinate system.

For some purposes we want to have an image of the whole detector, but retaining a link to the original chip pixels. The Tiled Detector (TDET) coordinates solve this problem by artificially laying the chips flat next to each other. There is no continuous world coordinate system that can be associated with the tiled detector coordinates.

At XRCF, the conversion between STF and HNC coordinates is not fixed, and may be dithered with time, which introduces several more intermediate systems. However, the sky pixel and celestial systems are not applicable, and data will end up in tangent plane coordinates.

Grating data requires some extra calculations using the HNC coordinates to obtain grating zero order (GZO) coordinates, dispersed grating coordinates (GDP) and ultimately the photon energy.

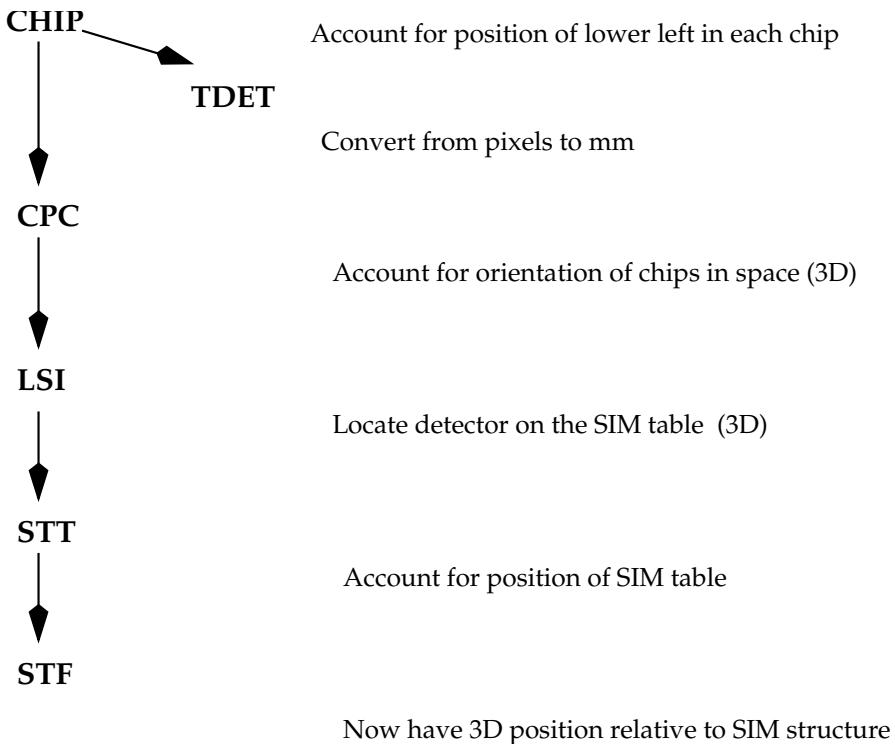

Figure 6: Coordinate systems used in data analysis, 1: Instrument related systems.

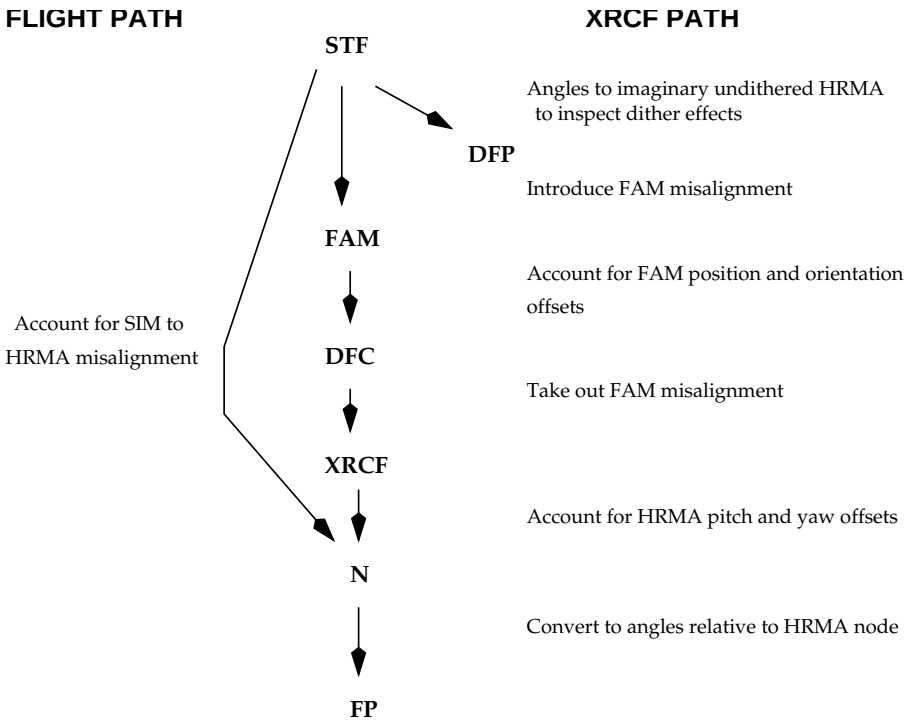

Figure 7: Coordinate systems used in data analysis, 2: Connecting the instrument to the HRMA.

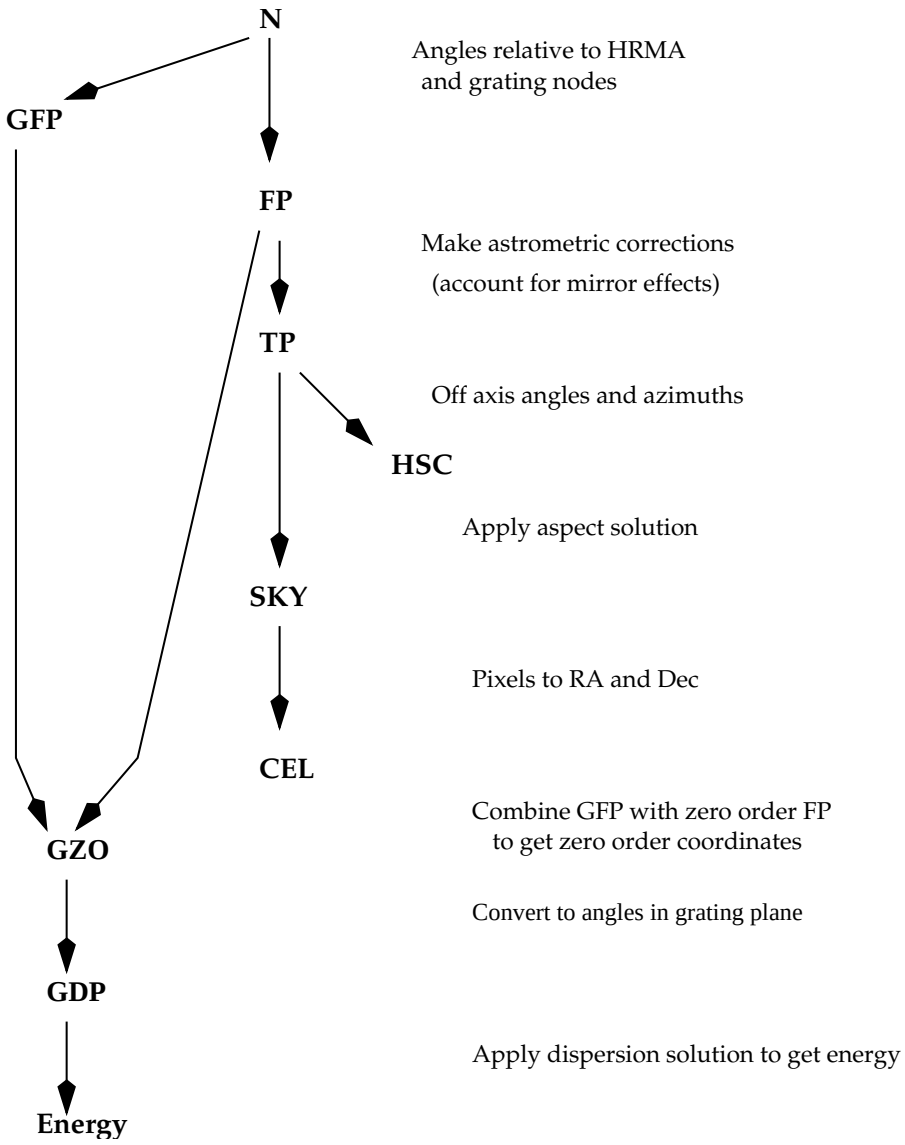

Figure 8: Coordinate systems used in data analysis, 3: From post-HRMA photon position to incoming photon properties.

2 Flight Data Analysis

In this section I describe the process of calculating the sky pixel coordinates from telemetered pixel numbers.

2.1 Coordinates for the detector chips

2.1.1 CHIP coordinates (DET-1.0)

We consider the AXAF detectors to be made up of collections of planar, finite rectangular 'chips' consisting of a rectangular array of XMAX by YMAX square pixels of equal physical size Δ_p on a side. These logical chips are positioned at various angles and locations in space to intersect photons coming from the HRMA or the gratings (e.g. for the HRC their spacecraft coordinates correspond to the surfaces of the MCPs, not of the wire grids). Note that parts of the logical chip may not correspond to a physical detector surface: an arbitrary subset of the pixels are specified to be 'active' and capable of detecting photons.

The pixel at one corner of the chip is labelled (1,1) and this corner is called the lower left corner (LL) of the chip; other pixels are numbered up to (XMAX, YMAX). This numbering scheme is extended to form a continuous, real valued coordinate system across the chip, **Chip coordinates** (CHIPX, CHIPY), in which the center of pixel (1,1) has coordinates (1.0, 1.0). The coordinates of LL (the lower left corner of the lower left pixel) are then (0.5, 0.5) and the coordinates of UR (the upper right corner of the rectangle) are (XMAX+0.5, YMAX+0.5).

The generic identifier for chip coordinates defined in this way is AXAF-DET-1.0, but the individual instruments have their own identifiers.

2.1.2 Chip Physical Coordinates (CPC-1.0)

We also lay down a three dimensional coordinate system, **Chip Physical Coordinates** $(X_{CPC}, Y_{CPC}, Z_{CPC})$ which have units of mm. The CPC X and Y axes are coincident with the chip X and Y axes, and the Z axis completes a right handed set. The CPC Z coordinate of any point in the chip has a value of 0.0. The X and Y coordinates run from 0.0 to XLEN and YLEN, where $XLEN = XMAX * \Delta_p$ and $YLEN = YMAX * \Delta_p$.

Thus if a photon lands at Chip Physical Coordinates X_{CPC}, Y_{CPC} its chip pixel coordinates are

$$\begin{aligned} CHIPX &= X_{CPC}/\Delta_p + 0.5 \\ CHIPY &= Y_{CPC}/\Delta_p + 0.5 \end{aligned} \tag{12}$$

or

$$\begin{aligned} X_{CPC} &= (CHIPX - 0.5)\Delta_p \\ Y_{CPC} &= (CHIPY - 0.5)\Delta_p \end{aligned} \tag{13}$$

Note that CHIPX and CHIPY are by definition linear, by which I mean that the mapping to real physical space is linear. Now for ACIS it so happens that the true CCD pixels satisfy this condition sufficiently accurately, but for HRC the readout values may require linearization.

2.1.3 Telemetry Pixel Numbers

The rawest form of coordinates in our data analysis are the telemetered pixel values. In ACIS data these correspond to the actual active area detector pixels, which are numbered from 0 to 1023 in x (column) and y (row). In HRC data, they are artificial; 256 pixels correspond approximately to the interval between two taps on the wire grids in the detector. In principle, the HRC-I detector returns pixel numbers from 0 to 16384 in the two axes, named u and v. The HRC-S detector returns numbers from 0 to 4096 in u and 0 to 16384 in v for each of three sets of grids. In practice, not all of those pixel values correspond to active areas of the detector and they do not match up with the edges of the microchannel plates which actually detect the photons. All the telemetered values have 1 added to them once they enter our data system, to match our convention of numbering pixels starting at 1.

2.1.4 ACIS CHIP coordinates (ACIS-1.0)

Each ACIS chip consists of an array of 1024 x 1024 pixels covering a 24.58 mm square. Thus, each pixel is 0.024mm on a side or 0.49 arcsec. There are two extra rows making 1024 x 1026, but they don't form part of the active area.

The ten ACIS chips have names and integer identifiers, listed in the table below.

Table 5: ACIS Chip Numbers

Chip Name	Chip ID
I0	0
I1	1
I2	2
I3	3
S0	4
S1	5
S2	6
S3	7
S4	8
S5	9

The chips calibrated so far have identities as follows; their mapping to the above table of flight chips is not yet determined.

Table 6: ACIS Chips

Chip	Type
W185C3	Front side
W163C1	Front side
W168C4	Front side
W190C1	Front side
W78C1	Front side
W147C3	Back side
W140C4	Back side
W134C4	Back side

The ACIS readout coordinate system was explained in a 1995 draft memo from J Woo. This memo defines two coordinate systems, the "pixel coordinate system of the readout file array, f(x,y)", which I will call the **ACIS Readout Coordinates** $(XREAD, YREAD)$ with identifier AXAF-ACIS-3.0, and the "pixel coordinate system of the active detector image array p(x,y)", which I will call **ACIS Chip Coordinates**, $(XCHIP, YCHIP)$ with identifier AXAF-ACIS-1.0 (these are the ones that run from 1 to 1024).

ACIS Readout Coordinates may be seen in subassembly cal (SAC) data, but in flight the Chip coordinates are calculated on board and telemetered directly. We don't normally deal with the readout coordinates.

The two systems are related by

$$YCHIP = \begin{cases} YREAD & 1 \leq YREAD \leq 1026 \\ \text{Overclock} & 1027 \leq YREAD \leq 1030 \end{cases} \tag{14}$$

$$XCHIP = \begin{cases} \text{Underclock} & 1 \le XREAD \le 4 & \\ XREAD - 4 & 5 \le XREAD \le 260 & \text{(Node A)} \\ \text{Overclock} & 261 \le XREAD \le 337 & \\ \text{Undefined Parallel Transfer} & 338 \le XREAD \le 340 & \\ \text{Underclock} & 341 \le XREAD \le 344 & \\ 857 - XREAD & 345 \le XREAD \le 600 & \text{(Node B} \\ \text{Overclock} & 601 \le XREAD \le 677 & \\ \text{Undefined Parallel Transfer} & 678 \le XREAD \le 680 & \\ \text{Underclock} & 681 \le XREAD \le 684 & \\ XREAD - 172 & 685 \le XREAD \le 940 & \text{(Node C)} \\ \text{Overclock} & 941 \le XREAD \le 1017 & \\ \text{Undefined Parallel Transfer} & 1018 \le XREAD \le 1020 & \\ \text{Underclock} & 1021 \le XREAD \le 1024 & \\ 2049 - XREAD & 1025 \le XREAD \le 1280 & \text{(Node D)} \\ \text{Overclock} & 1281 \le XREAD \le 1357 & \\ \text{Undefined Parallel Transfer} & 1358 \le XREAD \le 1360 & \end{cases} \tag{15}$$

The inverse transformation is

$$\begin{aligned} YREAD &= YCHIP \\ XREAD &= \begin{cases} XCHIP + 4 & 1 \le XCHIP \le 256 & \text{(A)} \\ 857 - XCHIP & 257 \le XCHIP \le 512 & \text{(B)} \\ XCHIP + 172 & 513 \le XCHIP \le 768 & \text{(C)} \\ 2049 - XCHIP & 769 \le XCHIP \le 1024 & \text{(D)} \end{cases} \end{aligned} \tag{16}$$

Unresolved questions: Is the above correct, or even useful? Do the telemetry values start at 1 or 0? Under what circumstances do we get YCHIP values of 1025 and 1026? Do those values correspond to true active area?

2.1.5 HRC physical layout and Tap Coordinates (HRC-6.0)

Each HRC sub-instrument contains a series of electrical 'taps' on each axis of the wire grid, which define a continuous spatial system. The electrical axes are labelled u and v, and we will say there are N_u and N_v taps on each axis, numbered starting at 0. In the internal HRC-S electronics the three MCPs have individually numbered taps but these are combined before we see it in the telemetry. The coarse tap positions are modified by a fine position which runs from -0.5 to +0.5. Then we can define an **HRC Tap Coordinate System** (AXAF-HRC-6.0) which runs from $u = -0.5$ to $u = N_u - 0.5$, and $v = -0.5$ to $N_v - 0.5$.

2.1.6 Deriving linear tap coordinates from HRC telemetry

The instrument electronics records four numbers per axis for each event: the 'center tap' (usually the tap with the maximum voltage), and the voltages of that tap and the one on either side. These

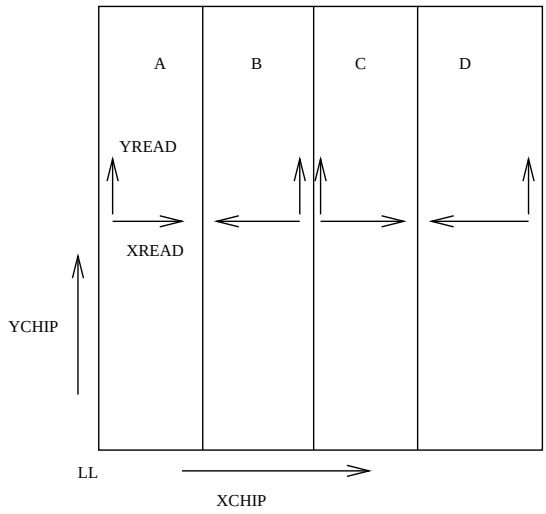

Figure 9: ACIS readout nodes

numbers, which are the values which get coded into flight telemetry, we will refer to as **HRC telemetry coordinates** $(\mathbf{u}_{ht}, \mathbf{v}_{ht})$. The four integer components of $\mathbf{u}_{ht}$ are

$$\mathbf{u}_{ht} = \begin{cases} u_0 & \text{Max tap, 0 to } N_u - 1 \text{ ('coarse position')} \\ \text{ADC1} & \text{Voltage of } u_{\text{coarse}} - 1 \\ \text{ADC2} & \text{Voltage of } u_{\text{coarse}} \\ \text{ADC3} & \text{Voltage of } u_{\text{coarse}} + 1 \end{cases} \tag{17}$$

and similarly for $\mathbf{v}_{ht}$). From the telemetry coordinates we can calculate an intermediate quantity, the **fine position**

$$u_{\text{fine}} = \frac{\text{ADC3} - \text{ADC1}}{\text{ADC1} + \text{ADC2} + \text{ADC3}} \tag{18}$$

Note that

$$-0.5 \le u_{\text{fine}} \le +0.5 \tag{19}$$

We now split off the sign of this fine position correction to obtain the tap side

$$s_u = \begin{cases} +1 & (u_{\text{fine}} \ge 0) \\ -1 & (u_{\text{fine}} < 0) \end{cases} \tag{20}$$

and the fine position magnitude

$$\Delta u = |u_{\text{fine}}| \tag{21}$$

From these we calculate the linear HRC Tap Coordinates

$$\begin{aligned} u &= u_0 + s_u C_{u1}(u_0, s_v)\Delta u - s_u C_{u2}(u_0, s)\Delta u^2 \\ v &= v_0 + s_v C_{v1}(v_0, s_v)\Delta v - s_v C_{v2}(v_0, s)\Delta v^2 \end{aligned} \tag{22}$$

The C factors are called the **degapping parameters**; for HRC they have different values for each tap and tap side. Earlier detectors (Einstein and Rosat HRI) assumed C factors which were independent of coarse position.

The simplest choice of the degapping parameters is to take

$$\begin{aligned} C_{u1} &= C_{v1} = 1 \\ C_{u2} &= C_{v2} = 0, \end{aligned} \tag{23}$$

giving us **HRC raw tap coordinates**,

$$\begin{aligned} u_{raw} &= (u_{\rm coarse} + u_{\rm fine}) \\ v_{raw} &= (v_{\rm coarse} + v_{\rm fine}) \end{aligned} \tag{24}$$

These coordinates do not provide a continuous system over the detector, and an HRC image plotted in raw coordinates contains 'gaps'. With some choice of the degapping parameters, we obtain a continuous (but not linear) system giving an image with no gaps. **HRC degapped coordinates** (u_{dg}, v_{dg}). Example values from Murray and Chappell (1989) of C used to give degapped coordinates are

$$\begin{aligned} C_{u1} &= C_{v1} = 1.049 \\ C_{u2} &= C_{v2} = 0.110, \end{aligned} \tag{25}$$

so

$$\begin{aligned} u_{dg} &= (u_{\rm coarse} + 1.049 u_{\rm fine} - 0.11 u_{\rm fine}|u_{\rm fine}|) \\ v_{dg} &= (v_{\rm coarse} + 1.049 v_{\rm fine} - 0.11 u_{\rm fine}|u_{\rm fine}|) \end{aligned} \tag{26}$$

The coefficients to be used for the HRC have not yet been determined.

2.1.7 HRC Chip Coordinates (HRC-1.1)

The HRC Telemetry Pixel Number System scales the taps by a pixel size $\Delta_t = 256$ to give

$$\begin{aligned} TELU &= (u + 0.5) * \Delta_t - 0.5 \\ TELV &= (v - v_0 + 0.5) * \Delta_t - 0.5, \end{aligned} \tag{27}$$

integer pixel numbers which start with pixel zero. The offset v_0 is 64.0 for HRC-S2, 128.0 for HRC-S3 and zero otherwise; it returns us to a system in which the taps are numbered separately for each chip.

For compatibility with other data archives, we add one to these engineering coordinates to get HRC Chip Coordinates (AXAF-HRC-1.0)

$$\begin{aligned} CHIPX &= (u + 0.5) * \Delta_t + 0.5 \\ CHIPY &= (v - v_0 + 0.5) * \Delta_t + 0.5 \end{aligned} \tag{28}$$

giving a system where the center of the first pixel has coordinate 1.0.

In this system, 1 pixel = 0.00643 mm = 0.13 arcsec. The size of one tap is 1.646mm. Now this coordinate system actually covers a larger area than the true possible coordinates. For instance, v taps 0 and 1 for HRC-S1 are missing, so the lowest possible v coordinate in the telemetry for HRC-S is 1.5 (corresponding to tap 2 with fine position -0.5) but even this does not correspond to a valid detected event position. Nevertheless, we will define our logical coordinate system to cover the full range of coordinates starting at CHIPX, CHIPY = 0.5 (lower left corner of first pixel). The previous version of this document defined chip coordinate system AXAF-HRC-1.0 which did not cover this full logical range and had a slightly different origin; the current system is denoted AXAF-HRC-1.1.

The center of HRC-S2 is then at $(u, v) = (7.5, 95.5)$ and the gaps between the MCPs are at v values of 62.96 to 64.12 and 124.88 to 126.04. I arbitrarily set the chip boundaries at 63.0 and 126.0 so that each chip has a length of 63.0 taps.

Table 7: HRC electronically meaningful coordinate ranges

Chip	v_0	u	v	CHIPX	CHIPY
HRC-I	0.0	0.0 to 63.0	0.0 to 63.0	0.5 to 16128.5	0.5 to 16128.5
HRC-S1	0.0	0.0 to 15.0	1.5 to 63.5	0.5 to 3840.5	384.5 to 16384.5
HRC-S2	64.0	0.0 to 15.0	-0.5 to 63.5	0.5 to 3840.5	0.5 to 16384.5
HRC-S3	128.0	0.0 to 15.0	-0.5 to 61.5	0.5 to 3840.5	0.5 to 15873.5

Now let's look at the boundaries on HRC-S and HRC-I more closely. We keep extra figures for self-consistency only assuming a tap scale of 1.6460 exactly, and measure positions starting at the physical position corresponding to chip pixel position 0.5 (bearing in mind this may be outside of the wire grid).

I used the following information on the HRC-S:

```
Tap size is 1.646 mm (M. Juda)
16384 pixels = 105.344 mm: logical chip size = tap size 1.646 mm x 64 taps
MCP physical size 100.000 mm x 27.000 mm from 'TOP MCP COORDINATES' drawing
Total logical length is 3 x 105.344 mm
Total physical length is 3 x 100.000 mm + 2 x gap size = 1.905 mm.
S2 Center is center of both total logical and total physical length.
Coating extends 94.5mm on outer MCPs and 16mm wide (M. Juda)
```

This information leads to the following MCP layout:

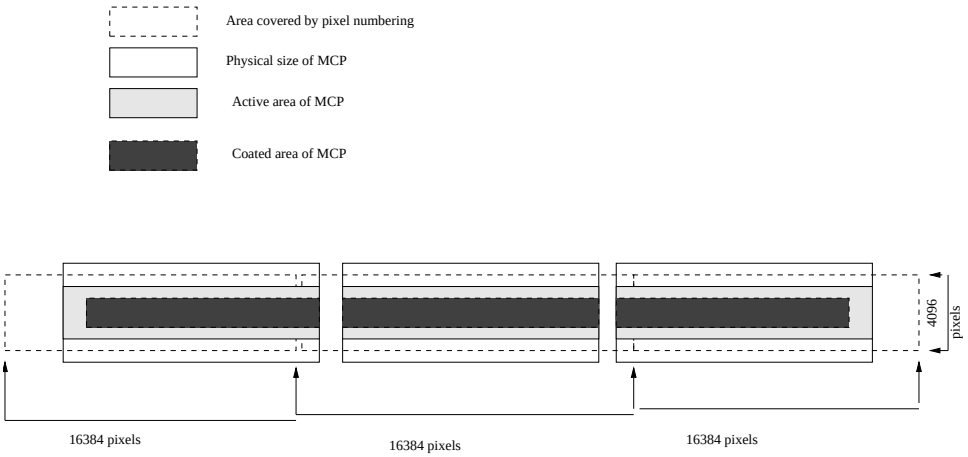

Figure 10: Relationship of HRC-S pixels to the physical instrument.

Table 8: HRC-S boundaries

Boundary	Tap v (AXAF-HRC-6.0)	Pos, mm	Seg No.	Y_{CPC}, mm (AXAF-CPC-1.0)	CHIPY, (AXAF-
S1 Logical Left Edge	-0.5	0.000	1	0.000	0.5
S1 Electronic Left Edge	1.50	3.292	1	3.292	512.5
S1 MCP Left Edge	3.21	6.111	1	6.111	950.3
S1 Coating Edge	6.55	11.611	1	11.611	1806.4
S1 Logical Right Edge	63.50	105.344	1	105.344	16384.5
S2 Logical Left Edge	63.50	105.344	2	0.000	0.5
S1 MCP Right Edge	63.97	106.111	2	0.767	119.8
S2 MCP Left Edge	65.12	108.016	2	2.672	416.1

S2 Center	95.50	158.016	2	52.672	8192.5
S2 MCP Right Edge	125.88	208.016	2	102.672	15968.9
S3 MCP Left Edge	127.03	209.921	2	104.577	16265.4
S2 Logical Right Edge	127.50	210.688	2	105.344	16384.5
S3 Logical Left Edge	127.50	210.688	3	0.000	0.5
S3 Coating Edge	184.45	304.421	3	93.733	14578.8
S3 MCP Right Edge	187.79	309.921	3	99.233	15434.2
S3 Electronic Right Edge	189.50	312.740	3	102.052	15872.6
S3 Logical Right Edge	191.50	316.032	3	105.344	16384.5

Boundary	Tap u	X_{CPC}, mm	CHIPX, pix
MCP Edge	-0.702	-0.332	-51.1
Logical Edge	-0.500	0.000	0.5
Active Area	1.425	3.168	493.3
Coating Edge	2.640	5.168	804.3
Center	7.500	13.168	2048.5
Coating Edge	12.360	21.168	3292.7
Active Area	13.575	23.168	3603.8
Logical Edge	15.500	26.336	4096.5
MCP Edge	15.702	26.668	4148.2

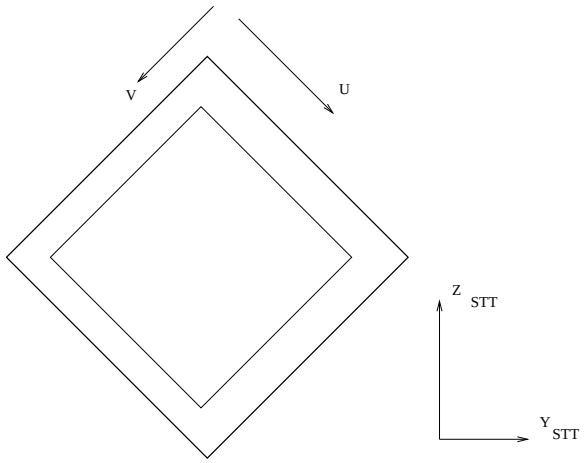

Figure 11: HRC-I pixel axes.

Table 9: HRC-I boundaries

Boundary	Tap u or v	X_{CPC} or Y_{CPC}, mm	CHIPX or CHIPY, pix
Logical Edge	-0.500	0.000	0.5
MCP Edge	1.123	2.672	416.1
Active Area	3.250	6.172	960.4
Coating Edge	4.161	7.672	1193.7
Center	31.500	52.672	8192.5
Coating Edge	58.839	97.672	15191.3
Active Area	59.750	99.172	15424.6
MCP Edge	61.877	102.672	15968.9
Logical Edge	63.500	105.344	16384.5

The CPC coordinates run from 0.0 to 26.33 (X_{CPC} for HRC-S) and from 0.0 to 105.3 (Y_{CPC} for HRC-S and both axes for HRC-I).

The active area of each microchannel plane is smaller, and the area coated with photocathode is smaller still. For HRC-I, the chip is 100 x 100 mm, with a 93 x 93 mm active area and a 90 x 90 mm coated area. For HRC-S, each chip is 100 x 27 mm, the active area is 100 x 20 mm, and the coated area is 94.5 x 16.0 mm. except for HRC-S2 where the coated area is 100 x 16 mm. Using these numbers, we derive the locations of the various areas in CPC (mm) and Chip (pixel) coordinates listed above.

2.2 Tiled Detector Coordinates (DET-2.0)

The AXAF detector chips do not lie in a plane; if we want to represent the detector as a whole, we can project from three dimensions to two and retain correct physical distances, but then the physical detector pixels do not have constant area in projected pixels, so we lose the information about which actual pixels were involved in detecting a photon. For many calibration purposes we wish to retain the information on individual chip pixels but look at all the chips at once on a flat image. In this case the detailed relative geometry of the chips is not important, and we can (in software) lay them flat next to each other. We choose to do this with the chips in approximately their correct relative orientation, but with the chip edges parallel and the gaps between the chips enlarged to be visible by inspection and chosen to be an integral number of pixels wide. This artificial tiling of the chips is accomplished in **Tiled Detector Coordinates**. The simplest transformation between Tiled Detector Coordinates and Chip pixel coordinates is a simple offset of an integer number of X and Y pixels for each chip. However, some of the chips are at 90 degrees to each other, so we may need to rotate X and Y. For HRC-I we may also want to rotate by 45 degrees (since their detector doesnt have real pixels we dont lose info by doing this), and we have to take into account that the chip coordinates have a different handedness than for the other detectors, in that a right-handed triad has its third axis to negative spacecraft X. And for ACIS we want to have integer pixels smaller

than the actual pixels to achieve maximum resolution. Units of Tiled Detector Coordinates are pixels.

$$\begin{pmatrix} DETX \\ DETY \end{pmatrix} = \Delta_i \begin{pmatrix} 1 & 0 \\ 0 & H_i \end{pmatrix} \begin{pmatrix} \cos\theta_i & \sin\theta_i \\ -\sin\theta_i & \cos\theta_i \end{pmatrix} \begin{pmatrix} CHIPX - 0.5 \\ CHIPY - 0.5 \end{pmatrix} + \begin{pmatrix} X0_i + 0.5 \\ Y0_i + 0.5 \end{pmatrix} \tag{29}$$

where the values of H_i, Δ_i and θ_i are different for each chip. H_i gives the handedness of the planar rotation and has values $+1$ or -1, Δ_i gives the sub-pixel resolution factor, and θ_i gives the rotation angle of the chip axes with respect to the detector coordinate axes.

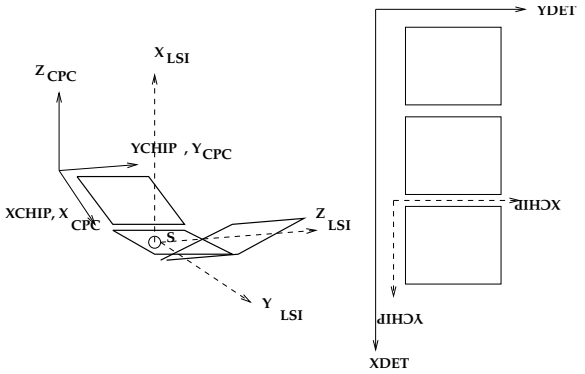

Figure 12: The relationship between CHIP and Tiled Detector coordinates.

Tiled Detector Coordinates are used for applying bad pixel maps, etc. Below I tablulate several alternative definitions of Tiled Detector Coordinates for each instrument. I have given two systems for HRC-S:

- HRC-2.2S places the chips next to each other with the gaps equal to their physical size, while
- HRC-2.1S places them one above the other to make a square picture (An earlier HRC-2.0S system had a mistake in it).

  I have defined a single tiled detector plane for the entire ACIS-I and ACIS-S combined instrument.

- AXAF-ACIS-2.2 defines a system centered on the ACIS-I detector. The chip coordinates of the ACIS-I nominal focus are estimated to be (61.3, 963.5) on ACIS-I1 with corresponding detector coordinates (4167.5, 4167.3).

- AXAF-ACIS-2.3 is identical to AXAF-ACIS-2.2 but shifted by 631 pixels in the DETX direction. The related system AXAF-ACIS-2.3A has pixels 5 times smaller ($\Delta_i = 5$) and will be used for handling XRCF data. For flight, I recommend that the ACIS-2.2 system be used and

sub-pixel resolution be addressed by keeping real-valued pixels when neccessary, and creating an image by using fractional-pixel bins if superresolution is desired. For XRCF, I recommend that ACIS-2.3A be used for storing short integer pixel locations in event lists; this allows us to store to sub-pixel precision within the current software limitations that restrict us to short integers. However, I recommend that for most purposes ACIS-2.3 with the true, coarser pixels should be used for creating images, by using a blocking factor of 5 (or multiple thereof).

- The AXAF-HRC-2.2I system rotates the HRC-I chip coordinates by 45 degrees to align the DETX, DETY axes with the SIM axes. It also restores the handedness of the coordinates to be the same as for the other detectors.

- The AXAF-HRC-2.3I system is provided as an alternative, involving less computation. The handedness of the axes is corrected, but the rotation is not applied and the resulting image is smaller.

The definitions of the tiled systems are given in terms of chip systems AXAF-ACIS-1.0 and AXAF-HRC-1.1.

Table 10: Tiled Detector Plane systems

System	Size	X Center, Y Center	Use
AXAF-ACIS-2.2	8192 x 8192	(4096.5, 4096.5)	Standard, Flight?
AXAF-ACIS-2.3A	32768x32768	(16384.5, 16384.5)	XRCF
AXAF-HRC-2.2I	32768 x 32768	(16384.5, 16384.5)	Standard
AXAF-HRC-2.3I	16384 x 16384	(8192.5, 8192.5)	Alternative
AXAF-HRC-2.2S	49152 x 4096	(24576.5, 2048.5)	Standard
AXAF-HRC-2.3S	16384 x 16384	(8192.5, 8192.5)	Alternative (and XRCF?)

Table 11: Parameters of Tiled Detector Coordinate definitions

Tiled System	Chip	θ_i	Δ_i	$X0_i$	$Y0_i$	H_i
AXAF-HRC-2.2I	HRC-I	315	1	16384.0	27969.2375	-1
AXAF-HRC-2.3I	HRC-I	90	1	0.0	0.0	-1
AXAF-HRC-2.2S	HRC-S1	270	1	49152.0	0.0	1
AXAF-HRC-2.2S	HRC-S2	270	1	32768.0	0.0	1
AXAF-HRC-2.2S	HRC-S3	270	1	16384.0	0.0	1

AXAF-HRC-2.3S	HRC-S1	270	1	16384.0	9216.0	1
AXAF-HRC-2.3S	HRC-S2	270	1	16384.0	14336.0	1
AXAF-HRC-2.3S	HRC-S3	270	1	16384.0	19456.0	1
AXAF-ACIS-2.2	ACIS-I0	90	1	3061.0	5131.0	1
AXAF-ACIS-2.2	ACIS-I1	270	1	5131.0	4107.0	1
AXAF-ACIS-2.2	ACIS-I2	90	1	3061.0	4085.0	1
AXAF-ACIS-2.2	ACIS-I3	270	1	5131.0	3061.0	1
AXAF-ACIS-2.2	ACIS-S0	0	1	791.0	1702.0	1
AXAF-ACIS-2.2	ACIS-S1	0	1	1833.0	1702.0	1
AXAF-ACIS-2.2	ACIS-S2	0	1	2875.0	1702.0	1
AXAF-ACIS-2.2	ACIS-S3	0	1	3917.0	1702.0	1
AXAF-ACIS-2.2	ACIS-S4	0	1	4959.0	1702.0	1
AXAF-ACIS-2.2	ACIS-S5	0	1	6001.0	1702.0	1
AXAF-ACIS-2.3	ACIS-I0	90	1	2430.0	5131.0	1
AXAF-ACIS-2.3	ACIS-I1	270	1	4500.0	4107.0	1
AXAF-ACIS-2.3	ACIS-I2	90	1	2430.0	4085.0	1
AXAF-ACIS-2.3	ACIS-I3	270	1	4500.0	3061.0	1
AXAF-ACIS-2.3	ACIS-S0	0	1	160.0	1702.0	1
AXAF-ACIS-2.3	ACIS-S1	0	1	1202.0	1702.0	1
AXAF-ACIS-2.3	ACIS-S2	0	1	2244.0	1702.0	1
AXAF-ACIS-2.3	ACIS-S3	0	1	3286.0	1702.0	1
AXAF-ACIS-2.3	ACIS-S4	0	1	4328.0	1702.0	1
AXAF-ACIS-2.3	ACIS-S5	0	1	5370.0	1702.0	1
AXAF-ACIS-2.3A	ACIS-I0	90	5	12150.0	25655.0	1
AXAF-ACIS-2.3A	ACIS-I1	270	5	22500.0	20535.0	1
AXAF-ACIS-2.3A	ACIS-I2	90	5	12150.0	20425.0	1
AXAF-ACIS-2.3A	ACIS-I3	270	5	22500.0	15305.0	1
AXAF-ACIS-2.3A	ACIS-S0	0	5	800.0	8510.0	1
AXAF-ACIS-2.3A	ACIS-S1	0	5	6010.0	8510.0	1
AXAF-ACIS-2.3A	ACIS-S2	0	5	11220.0	8510.0	1
AXAF-ACIS-2.3A	ACIS-S3	0	5	16430.0	8510.0	1
AXAF-ACIS-2.3A	ACIS-S4	0	5	21640.0	8510.0	1
AXAF-ACIS-2.3A	ACIS-S5	0	5	26850.0	8510.0	1

Table 12: Coordinates of Nominal Focus Position

Instrument	DET System	DETX, DETY	CHIPX, CHIPY	DET_ID
ACIS-I AI1	AXAF-ACIS-2.3A	(17687.5, 16744.5)	(61.3, 963.3)	ACIS-I1
ACIS-I AI2	AXAF-ACIS-2.3A	(17687.5, 16014.5)	(961.7, 963.3)	ACIS-I3
ACIS-S	AXAF-ACIS-2.3A	(17686.5, 6972.5)	(251.9, 512.5)	ACIS-S3
ACIS-I AI1	AXAF-ACIS-2.2	(4168.7, 4168.3)	(61.3, 963.3)	ACIS-I1
ACIS-I AI2	AXAF-ACIS-2.2	(4168.7, 4022.7)	(961.7, 963.3)	ACIS-I3
ACIS-S	AXAF-ACIS-2.2	(4168.9, 2214.5)	(251.9, 512.5)	ACIS-S3
HRC-I	AXAF-HRC-2.1I	(16384.5, 16384.5)	(8192.5, 8192.5)	HRC-I
HRC-S	AXAF-HRC-2.2S	(23954.8, 2048.5)	(2048.5, 8814.2)	HRC-S2
HRC-S	AXAF-HRC-2.3S	(7570.8, 16384.5)	(2048.5, 8814.2)	HRC-S2

2.3 Three dimensional location of detector pixels

2.3.1 Local Science Instrument coordinates (LSI-1.1)

The next step in data analysis is to account for the orientations of the tilted chips in three dimensional space. Local Science Instrument (LSI) coordinates (basically the Focal Plane Science Instruments frame of TRW D17388) allow us to describe positions in three dimensions relative to the nominal aimpoint on one of the science instruments (ACIS-I, ACIS-S, HRC-I or HRC-S). The LSI frame axes are lined up with the spacecraft and HRMA nodal axes (in the nominal configuration) but are fixed in the science instrument (SI). Each instrument has a nominal aimpoint S (ACIS has two, but I adopt AI1 as the default one) which serves as the origin of the LSI frame (X_L, Y_L, Z_L). The X-axis is normal to the detector, with the Y axis in the dispersion direction and the Z axis along the translation direction, so that they are coincident with the HRMA and spacecraft Y and Z axes when everything is lined up in the usual way.

Note that the image falling on the chip is inverted so that on the final reconstructed image a 'lower left' corner will actually be in the upper right. (Is that correct?).

The transformation between CPC and LSI coordinates is defined by specifying the CPC and LSI coordinates of each of the four corners of the chip.

In going from an incident ray vector to a CPC pixel position we need to determine the intersection of the ray line and the pixel plane. Let's consider a set of position vectors with origin at $\boldsymbol{S}$ (i.e. working in the LSI frame).

A general point on the plane is

$$\boldsymbol{r} = \boldsymbol{p_0} + X_{CPC}\boldsymbol{e}_X + Y_{CPC}\boldsymbol{e}_Y \tag{30}$$

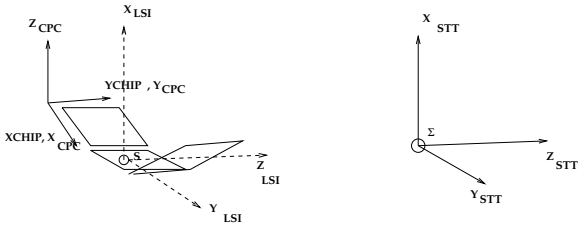

Figure 13: The relationship between CHIP, LSI and STT coordinates.

where $\boldsymbol{p_0}$ is the origin of CPC coordinates, and $\boldsymbol{e}_X$ and $\boldsymbol{e}_Y$ are the unit vectors along the CPC axes, with $\boldsymbol{e}_Z$ as the unit normal to the plane.

This immediately gives the LSI coordinates, and hence the HRMA nodal coordinates, of a point on the chip, which we can use to find the off-axis angle by converting to HRMA spherical coordinates, and hence the direction of the incoming photon.

We can recast this in our usual rotational formulation,

$$P_{LSI}(G) = P_{LSI}(LL) + R(CPC, LSI)P_{CPC}(G) \tag{31}$$

where the matrix is

$$R(CPC, LSI) = \begin{pmatrix} (\boldsymbol{e_X})_X & (\boldsymbol{e_Y})_X & (\boldsymbol{e_Z})_X \\ (\boldsymbol{e_X})_Y & (\boldsymbol{e_Y})_Y & (\boldsymbol{e_Z})_Y \\ (\boldsymbol{e_X})_Z & (\boldsymbol{e_Y})_Z & (\boldsymbol{e_Z})_Z \end{pmatrix} \tag{32}$$

The reverse process (CPC coordinates from incident photon) is a little harder. The general ray is

$$\boldsymbol{r} = \boldsymbol{l_0} + \lambda \boldsymbol{l} \tag{33}$$

where $\boldsymbol{l_0}$ is an arbitrary point on the ray, $\boldsymbol{l}$ is the ray direction, and λ labels positions along the ray. The intersection with the plane is then at

$$\boldsymbol{r} = \boldsymbol{l_0} + \frac{(\boldsymbol{p_0} - \boldsymbol{l_0}).\boldsymbol{e}_Z}{\boldsymbol{l}.\boldsymbol{e}_Z}\boldsymbol{l} \tag{34}$$

and we find CPC X and Y by taking the dot product with the unit vectors,

$$X_{CPC} = \boldsymbol{r}.\boldsymbol{e}_X, \quad Y_{CPC} = \boldsymbol{r}.\boldsymbol{e}_Y \tag{35}$$

Let us denote the position vectors of the four chip corners as $\boldsymbol{LL}$,$\boldsymbol{UL}$,$\boldsymbol{UR}$,$\boldsymbol{LR}$. Then

$$\boldsymbol{p_0} = \boldsymbol{LL}, \boldsymbol{e}_X = \boldsymbol{LR} - \boldsymbol{LL}, \boldsymbol{e}_Y = \boldsymbol{UL} - \boldsymbol{LL} \tag{36}$$

and

$$\boldsymbol{e}_Z = \boldsymbol{e}_X \wedge \boldsymbol{e}_Y. \tag{37}$$

In the following tables we list the coordinates of each corner of each chip. We give coordinates for each of the ACIS chips in both the ACIS-I and ACIS-S LSI systems, since we may take data from ACIS-S chips while ACIS-I is in the focus or vice versa. The systems are simply offset by 46.88mm in the Z_{LSI} direction. The ACIS data is from ACIS-SOP-01, and the HRC data is deduced from information provided by M. Juda.

Table 13: ACIS Chip corner locations in ACIS-I LSI coordinates

Chip	Corner	CPC coords	ACIS-I LSI coords
I0	LL	(0.0, 0.0, 0.0)	(2.361, -26.484, 23.088)
	LR	(24.58, 0.0, 0.0)	(1.130, -26.546, -1.458)
	UR	(24.58, 24.58, 0.0)	(-0.100, -2.001, -1.458)
	UL	(0.0, 24.58, 0.0)	(1.130, -1.939, 23.088)
I1	LL	(0.0, 0.0, 0.0)	(1.130, 23.086, -1.458)
	LR	(24.58, 0.0, 0.0)	(2.360, 23.024, 23.088)
	UR	(24.58, 24.58, 0.0)	(1.130, -1.521, 23.088)
	UL	(0.0, 24.58, 0.0)	(-0.100, -1.459, -1.458)
I2	LL	(0.0, 0.0, 0.0)	(1.130, -26.546, -1.997)
	LR	(24.58, 0.0, 0.0)	(2.361, -26.484, -26.543)
	UR	(24.58, 24.58, 0.0)	(1.130, -1.939, -26.543)
	UL	(0.0, 24.58, 0.0)	(-0.100, -2.001, -1.997)
I3	LL	(0.0, 0.0, 0.0)	(2.361, 23.024, -26.543)
	LR	(24.58, 0.0, 0.0)	(1.131, 23.086, -1.997)
	UR	(24.58, 24.58, 0.0)	(-0.100, -1.459, -1.997)
	UL	(0.0, 24.58, 0.0)	(1.130, -1.521, -26.543)
S0	LL	(0.0, 0.0, 0.0)	(0.744, -81.051, -59.170)
	LR	(24.58, 0.0, 0.0)	(0.353, -56.478, -59.170)
	UR	(24.58, 24.58, 0.0)	(0.353, -56.478, -34.590)
	UL	(0.0, 24.58, 0.0)	(0.744, -81.051, -34.590)
S1	LL	(0.0, 0.0, 0.0)	(0.348, -56.047, -59.170)
	LR	(24.58, 0.0, 0.0)	(0.099, -31.473, -59.170)
	UR	(24.58, 24.58, 0.0)	(0.099, -31.473, -34.590)
	UL	(0.0, 24.58, 0.0)	(0.348, -56.047, -34.590)
S2	LL	(0.0, 0.0, 0.0)	(0.096, -31.042, -59.170)
	LR	(24.58, 0.0, 0.0)	(-0.011, -6.466, -59.170)
	UR	(24.58, 24.58, 0.0)	(-0.011, -6.466, -34.590)
	UL	(0.0, 24.58, 0.0)	(0.096, -31.042, -34.590)
S3	LL	(0.0, 0.0, 0.0)	(-0.011, -6.035, -59.170)
	LR	(24.58, 0.0, 0.0)	(0.024, 18.541, -59.170)
	UR	(24.58, 24.58, 0.0)	(0.024, 18.541, -34.590)

	UL	(0.0, 24.58, 0.0)	(-0.011, -6.035, -34.590)
S4	LL	(0.0, 0.0, 0.0)	(0.026, 18.972, -59.170)
	LR	(24.58, 0.0, 0.0)	(0.208, 43.547, -59.170)
	UR	(24.58, 24.58, 0.0)	(0.208, 43.547, -34.590)
	UL	(0.0, 24.58, 0.0)	(0.026, 18.972, -34.590)
S5	LL	(0.0, 0.0, 0.0)	(0.208, 43.978, -59.170)
	LR	(24.58, 0.0, 0.0)	(0.528, 68.552, -59.170)
	UR	(24.58, 24.58, 0.0)	(0.528, 68.552, -34.590)
	UL	(0.0, 24.58, 0.0)	(0.208, 43.978, -34.590)

Table 14: ACIS chip corner locations in ACIS-S LSI coordinates

Chip	Corner	CPC coords	ACIS-S LSI coords
I0	LL	(0.0, 0.0, 0.0)	(2.361, -26.484, 69.968)
	LR	(24.58, 0.0, 0.0)	(1.130, -26.546, 45.422)
	UR	(24.58, 24.58, 0.0)	(-0.100, -2.001, 45.422)
	UL	(0.0, 24.58, 0.0)	(1.130, -1.939, 69.968)
I1	LL	(0.0, 0.0, 0.0)	(1.130, 23.086, 45.422)
	LR	(24.58, 0.0, 0.0)	(2.360, 23.024, 69.968)
	UR	(24.58, 24.58, 0.0)	(1.130, -1.521, 69.968)
	LL	(0.0, 24.58, 0.0)	(-0.100, -1.459, 45.422)
I2	LL	(0.0, 0.0, 0.0)	(1.130, -26.546, 44.883)
	LR	(24.58, 0.0, 0.0)	(2.361, -26.484, 20.337)
	UR	(24.58, 24.58, 0.0)	(1.130, -1.939, 20.337)
	UL	(0.0, 24.58, 0.0)	(-0.100, -2.001, 44.883)
I3	LL	(0.0, 0.0, 0.0)	(2.361, 23.024, 20.337)
	LR	(24.58, 0.0, 0.0)	(1.131, 23.086, 44.883)
	UR	(24.58, 24.58, 0.0)	(-0.100, -1.459, 44.883)
	UL	(0.0, 24.58, 0.0)	(1.130, -1.521, 20.337)
S0	LL	(0.0, 0.0, 0.0)	(0.744, -81.051, -12.290)
	LR	(24.58, 0.0, 0.0)	(0.353, -56.478, -12.290)
	UR	(24.58, 24.58, 0.0)	(0.353, -56.478, 12.290)
	UL	(0.0, 24.58, 0.0)	(0.744, -81.051, 12.290)
S1	LL	(0.0, 0.0, 0.0)	(0.348, -56.047, -12.290)
	LR	(24.58, 0.0, 0.0)	(0.099, -31.473, -12.290)
	UR	(24.58, 24.58, 0.0)	(0.099, -31.473, 12.290)
	UL	(0.0, 24.58, 0.0)	(0.348, -56.047, 12.290)
S2	LL	(0.0, 0.0, 0.0)	(0.096, -31.042, -12.290)
	LR	(24.58, 0.0, 0.0)	(-0.011, -6.466, -12.290)
	UR	(24.58, 24.58, 0.0)	(-0.011, -6.466, 12.290)
	UL	(0.0, 24.58, 0.0)	(0.096, -31.042, 12.290)
S3	LL	(0.0, 0.0, 0.0)	(-0.011, -6.035, -12.290)
	LR	(24.58, 0.0, 0.0)	(0.024, 18.541, -12.290)
	UR	(24.58, 24.58, 0.0)	(0.024, 18.541, 12.290)

	UL	(0.0, 24.58, 0.0)	(-0.011, -6.035, 12.290)
S4	LL	(0.0, 0.0, 0.0)	(0.026, 18.972, -12.290)
	LR	(24.58, 0.0, 0.0)	(0.208, 43.547, -12.290)
	UR	(24.58, 24.58, 0.0)	(0.208, 43.547, 12.290)
	UL	(0.0, 24.58, 0.0)	(0.026, 18.972, 12.290)
S5	LL	(0.0, 0.0, 0.0)	(0.208, 43.978, -12.290)
	LR	(24.58, 0.0, 0.0)	(0.528, 68.552, -12.290)
	UR	(24.58, 24.58, 0.0)	(0.528, 68.552, 12.290)
	UL	(0.0, 24.58, 0.0)	(0.208, 43.978, 12.290)

Table 15: HRC chip (i.e. grid) corner locations in LSI coordinates

Chip	Corner	CPC coords	HRC-I,S LSI coords
HRC-I	LL	(0.000 , 0.000 , 0.000)	(0.000 , 0.000 , 74.489)
HRC-I	LR	(105.344 , 0.000 , 0.000)	(0.000 , 74.489 , 0.000)
HRC-I	UR	(105.344 , 105.344 , 0.000)	(0.000 , 0.000 , -74.490)
HRC-I	UL	(0.000 , 105.344 , 0.000)	(0.000 , -74.489 , 0.000)
HRC-S1	LL	(0.000 , 0.000 , 0.000)	(2.622 , 161.984 , -13.168)
HRC-S1	LR	(26.336 , 0.000 , 0.000)	(2.622 , 161.984 , 13.168)
HRC-S1	UR	(26.336 , 105.344 , 0.000)	(0.000 , 56.672 , 13.168)
HRC-S1	UL	(0.000 , 105.344 , 0.000)	(0.000 , 56.672 , -13.168)
HRC-S2	LL	(0.000 , 0.000 , 0.000)	(0.000 , 56.672 , -13.168)
HRC-S2	LR	(26.336 , 0.000 , 0.000)	(0.000 , 56.672 , 13.168)
HRC-S2	UR	(26.336 , 105.344 , 0.000)	(0.000 , -48.672 , 13.168)
HRC-S2	UL	(0.000 , 105.344 , 0.000)	(0.000 , -48.672 , -13.168)
HRC-S3	LL	(0.000 , 0.000 , 0.000)	(0.000 , -48.671 , -13.168)
HRC-S3	LR	(26.336 , 0.000 , 0.000)	(0.000 , -48.671 , 13.168)
HRC-S3	UR	(26.336 , 105.344 , 0.000)	(2.248 , -153.991 , 13.168)
HRC-S3	UL	(0.000 , 105.344 , 0.000)	(2.248 , -153.991 , -13.168)

The following table gives the Euler rotation angles for the chips. The LSI to CPC transformation is more intuitive; the first angle ϕ indicates the tilt with respect to the LSI plane (with HRC-I having $\phi = 180$ to indicate being completely flipped over, another way of expressing the different handedness of its axes); and the third angle ψ indicates the rotation of the chip in the LSI Y,Z plane relative to chip I0.

Table 16: Euler angles in degrees for CPC to LSI coordinates

Chip	CPC to LSI	LSI to CPC
I0	Rot(180, 92.875, 177.129)	Rot(2.871, 92.875, 0.0)
I1	Rot(0, 92.872, 182.869)	Rot(-2.869, 92.872, 180.0)
I2	Rot(180, 87.125, 177.131)	Rot(2.869, 87.125, 0.0)
I3	Rot(0, 87.128, 182.871)	Rot(-2.871, 87.128, 180.0)
S0	Rot(90.0, 90.0, 179.088)	Rot(0.912, 90.0, 90.0)
S1	Rot(90.0, 90.0, 179.419)	Rot(0.581, 90.0, 90.0)

S2	Rot(90.0, 90.0, 179.751)	Rot(0.249, 90.0, 90.0)
S3	Rot(90.0, 90.0, 180.082)	Rot(-0.082, 90.0, 90.0)
S4	Rot(90.0, 90.0, 180.424)	Rot(-0.424, 90.0, 90.0)
S5	Rot(90.0, 90.0, 180.746)	Rot(-0.746, 90.0, 90.0)
HRC-I	Rot(-135.0, 90.0, 0.0)	Rot(180.0, 90.0, -45.0)
HRC-S1	Rot(0.0, 90.0, 181.426)	Rot(-1.426, 90.0, 180.0)
HRC-S2	Rot(0.0, 90.0, 180.0)	Rot(0.0, 90.0, 180.0)
HRC-S3	Rot(0.0, 90.0, 178.778)	Rot(1.222, 90.0, 180.0)

For the record, the positions of the physical edges of the HRC MCPs, from which the grid edges were deduced, are given in an appendix.

The HRC chip corner data was derived from a drawing supplied by A. McKay. It has been assumed that the coordinates given in that drawing are effectively HRC-I LSI coordinates but measured in inches.

2.3.2 The SIM Translation Table Frame (STT-1.0)

Our next step is to locate the instruments relative to one another. The SIs are rigidly mounted to the SIM Translation Table, which is mounted either in the spacecraft or (at XRCF) on the FAM. We specify the relative positions of the SIs to each other in SIM Translation Table (STT) coordinates which are fixed in the SIM Translation Table. Each SI has its own nominal focal point S, and local coordinate system with origin at that focal point. The SI local coordinate systems (LSI frames) are parallel to each other and to the STT frame, with a simple origin offset. STT coordinates are also called SIM coordinates, but so are STF coordinates described below, so I don't use 'SIM coordinates' to avoid ambiguity. STT coordinates $(X_{STT}, Y_{STT}, Z_{STT})$ describe the locations of objects attached to the SIM.

In earlier versions of this memo the nominal position of the SIM was defined to be the AS1 aimpoint; however I now use the SIM coordinate system origin defined in drawing E445944 (1996 Mar 15) instead of that in [1], drawing 301438 (1995 Aug 31).

Each SI (ACIS-I, ACIS-S, HRC-I, HRC-S) has its own nominal focus position, which is defined in the SIM Translation Table (STT) coordinate system. The STT coordinates of a point may be found from its LSI coordinates by

$$\begin{pmatrix} X_{STT} \\ Y_{STT} \\ Z_{STT} \end{pmatrix} = \begin{pmatrix} X_L \\ Y_L \\ Z_L \end{pmatrix} + \begin{pmatrix} X_{STT}(S) \\ Y_{STT}(S) \\ Z_{STT}(S) \end{pmatrix} \tag{38}$$

Here are the STT coordinates for the nominal focus positions:

Table 17: SIM position offsets for nominal focus positions

Values of $P_{STT}(S)$, i.e. offsets $S - \Sigma$	
AI1 ACIS-I offset	(0.0, 0.0, 237.4)
AI2 ACIS-I offset	(0.0, 0.0, 233.9)
AS1 ACIS-S offset	(0.0, 0.0, 190.5)
HI1 HRC-I offset	(0.15, 0.0, -126.6)
HS1 HRC-S offset	(0.10, 0.0, -250.1)

The LSI origins are at AI1, AS1, HI1 and HS1. AI2 is a reserve ACIS aimpoint. The offsets in the X direction are taken from the Obs/SI ICD [1], Appendix A, p.2.

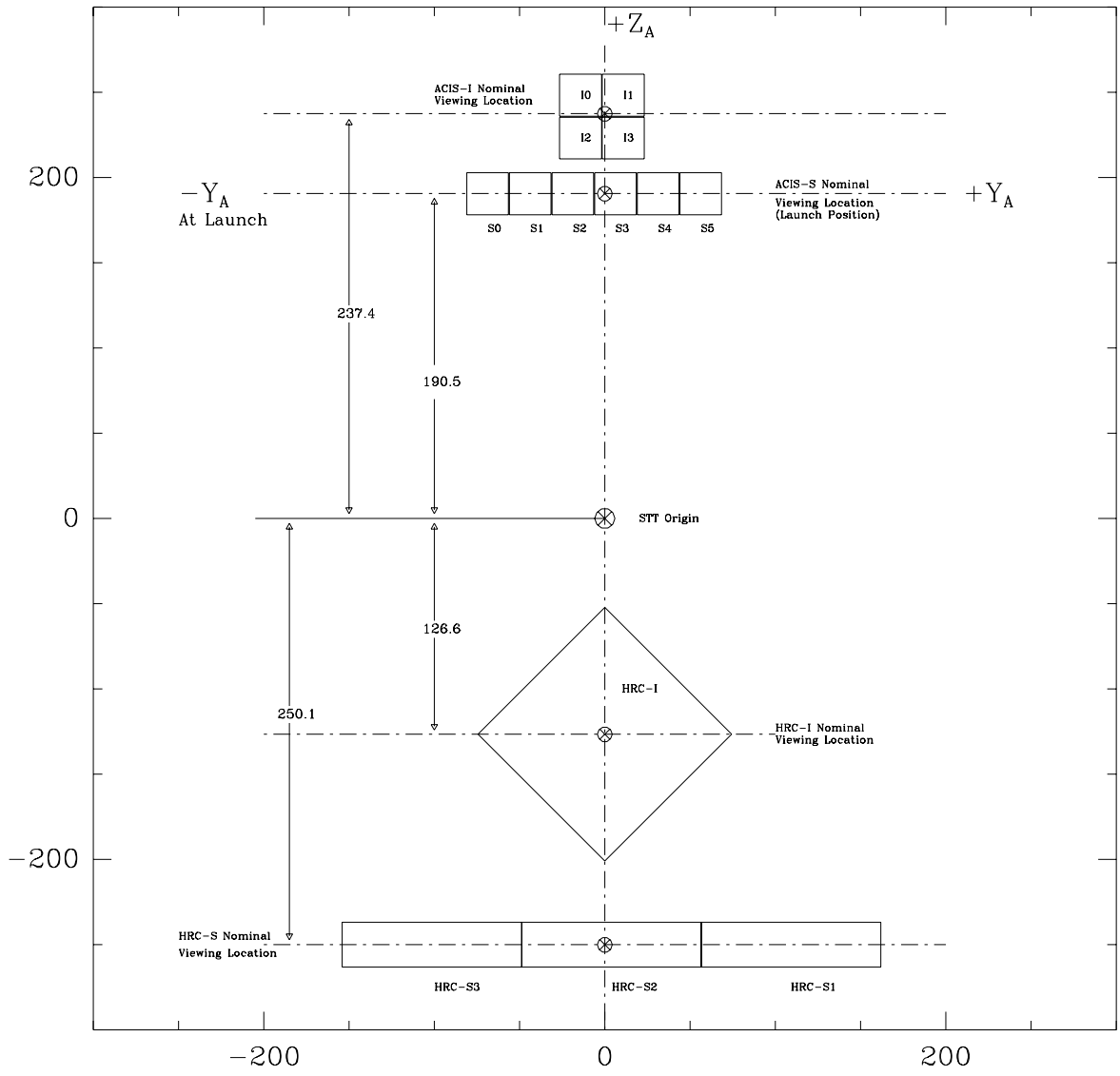

Figure 14: Scale drawing of the (Y_{STT}, Z_{STT}) plane showing relative positions of instruments.

2.3.3 SIM Travel Frame coordinates

We now define an intermediate coordinate system $(X_{STF}, Y_{STF}, Z_{STF})$ called the SIM Travel Frame. We describe the motion of the SIM in this frame, which is coincident with the SIM frame (see below) when the SIM is at its nominal position. In flight the SIM Travel Frame is just an offset from HRMA nodal coordinates, but at XRCF the SIM Travel Frame may be at an arbitrary orientation and origin offset with respect to the HRMA, and is our key to determining the dither solution. In flight, the SIM axes are parallel to the HRMA axes, and when the SIM is at its nominal position Σ_0 the Y,Z axes of SIM and HRMA coincide. As the SIM table moves, the coordinates of Σ in the SIM Travel Frame change, and so do the coordinates of an arbitrary point fixed to the STT:

$$\begin{pmatrix} X_{STF} \\ Y_{STF} \\ Z_{STF} \end{pmatrix} = \begin{pmatrix} X_{STT} \\ Y_{STT} \\ Z_{STT} \end{pmatrix} + \begin{pmatrix} X_{STF}(\Sigma) \\ Y_{STF}(\Sigma) \\ Z_{STF}(\Sigma) \end{pmatrix} \tag{39}$$

Combining this with the LSI to STT translation we derive

$$\begin{pmatrix} X_{STF} \\ Y_{STF} \\ Z_{STF} \end{pmatrix} = \begin{pmatrix} X_L \\ Y_L \\ Z_L \end{pmatrix} + \begin{pmatrix} X_{STT}(S) \\ Y_{STT}(S) \\ Z_{STT}(S) \end{pmatrix} + \begin{pmatrix} X_{STF}(\Sigma) \\ Y_{STF}(\Sigma) \\ Z_{STF}(\Sigma) \end{pmatrix} \tag{40}$$

These two offsets from LSI coordinates are the offset from the SI aimpoint to the SIM table origin and the offset of the SIM table origin from the SIM axis. Normally we move the SIM table so that these offsets cancel, and the SI aimpoint is on the SIM axis (which should also be the telescope optical axis). Thus in normal use LSI and STF coordinates are identical and we don't have to bother with STT and STF at all. But this won't always be true, for instance if we observe with ACIS alternate aimpoint AI2.

Note: The STF frame is a simple offset from the SIM coordinate frame defined in TRW D17388, which has an inconvenient origin and units, and a confusing name:

$$\begin{pmatrix} X_{STF} \\ Y_{STF} \\ Z_{STF} \end{pmatrix} = 25.4 * \begin{pmatrix} X_{SIM} + 28.5 \\ Y_{SIM} \\ Z_{SIM} \end{pmatrix} \tag{41}$$

2.3.4 HRMA Nodal Coordinates (HNC)

We have located the event pixel relative to the SIM structure; we must now locate it relative to the telescope mirror, the HRMA. In particular, for data analysis we want to know the photon's trajectory from the HRMA Node, the apparent position from which the photons emanate. HRMA Nodal Coordinates (X_N, Y_N, Z_N) have their origin at the HRMA node and axes parallel to the

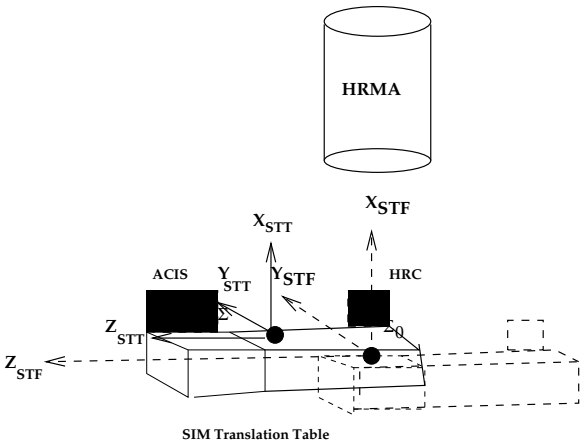

Figure 15: The relationship between STT and STF coordinates. The SIM table has moved so that HRC is at the focus.

spacecraft axes. Thus, positive X is towards the source. In flight, ideally the difference between STF and HNC is just an offset by the focal length along the X axis:

$$\begin{pmatrix} X_{STF} \\ Y_{STF} \\ Z_{STF} \end{pmatrix} + \begin{pmatrix} f \\ 0 \\ 0 \end{pmatrix} = \begin{pmatrix} X_N \\ Y_N \\ Z_N \end{pmatrix} \tag{42}$$

but there may be an alignment rotation matrix. (At XRCF there is no telescope structure and the conversion from STF to HNC coordinates does require a general translation and rotation.) HNC coordinates will be discussed further below.

In the nominal configuration on orbit, with the SI aimpoint on axis,

$$\begin{pmatrix} X_L \\ Y_L \\ Z_L \end{pmatrix} = \begin{pmatrix} X_N \\ Y_N \\ Z_N \end{pmatrix} + \begin{pmatrix} f \\ 0 \\ 0 \end{pmatrix} \tag{43}$$

When the roll angle is zero, photons with larger RA land on the detector at lower values of Y_L, while photons from higher Dec than the on-axis value land at negative Z_L.

In a general flight configuration, what are the HRMA nodal coordinates of a point $\boldsymbol{G}$ given in LSI coordinates?

- The LSI coordinates give $\boldsymbol{G}$ relative to $\boldsymbol{S}$, the detector nominal focus position;
- The table below gives $\boldsymbol{S}$ relative to $\boldsymbol{\Sigma}$, locating the detector on the translation table;
- The current SIM position gives $\boldsymbol{\Sigma}$ relative to $\boldsymbol{\Sigma_0}$, describing the state of the translation table;

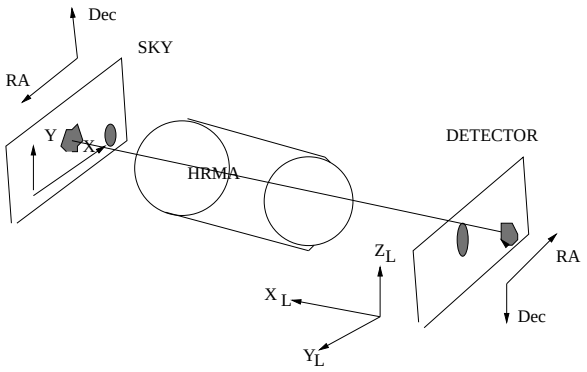

Figure 16: Imaging the sky in LSI coordinates

- and since we are in flight, $\mathbf{\Sigma_0}$ coincides with $\boldsymbol{F}$, the telescope focus, so we can get the nodal coordinates.

$$P_N(G) = P_N(F) + P_{STF}(\Sigma) + P_{STT}(S) + P_L(G) \tag{44}$$

or in detail

$$\begin{aligned}
\begin{pmatrix} X_N \\ Y_N \\ Z_N \end{pmatrix} &= \begin{pmatrix} -f \\ 0 \\ 0 \end{pmatrix} + \begin{pmatrix} X_{STF} \\ Y_{STF} \\ Z_{STF} \end{pmatrix} \\
&= \begin{pmatrix} -f \\ 0 \\ 0 \end{pmatrix} + \begin{pmatrix} X_{STF}(\Sigma) \\ Y_{STF}(\Sigma) \\ Z_{STF}(\Sigma) \end{pmatrix} + \begin{pmatrix} X_{STT} \\ Y_{STT} \\ Z_{STT} \end{pmatrix} \\
&= \begin{pmatrix} -f \\ 0 \\ 0 \end{pmatrix} + \begin{pmatrix} X_{STF}(\Sigma) \\ Y_{STF}(\Sigma) \\ Z_{STF}(\Sigma) \end{pmatrix} + \begin{pmatrix} X_{STT}(S) \\ Y_{STT}(S) \\ Z_{STT}(S) \end{pmatrix} + \begin{pmatrix} X_L \\ Y_L \\ Z_L \end{pmatrix}
\end{aligned} \tag{45}$$

Usually we don't have to bother with this since the SIM is usually moved to the appropriate focus position for the instrument, which is defined by

$$\begin{pmatrix} X_{STF}(\Sigma) \\ Y_{STF}(\Sigma) \\ Z_{STF}(\Sigma) \end{pmatrix} + \begin{pmatrix} X_{STT}(S) \\ Y_{STT}(S) \\ Z_{STT}(S) \end{pmatrix} = 0. \tag{46}$$

This recovers the nominal configuration.

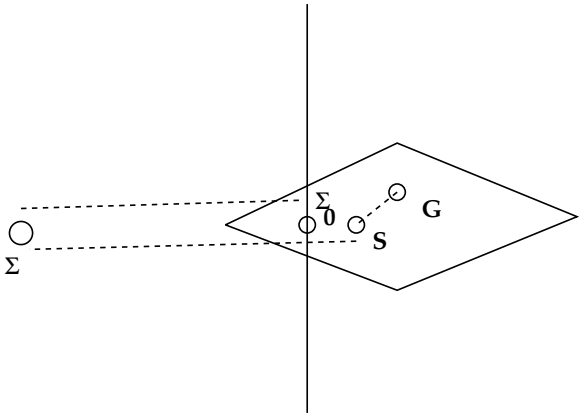

Figure 17: Correcting LSI coordinates for SIM position

2.4 Focal and Tangent plane systems

2.4.1 Focal Plane Pixel Coordinates

We define Focal Plane Pixel Coordinates by

$$\begin{aligned} FPX &= FPX0 - \Delta_s^{-1}(Y_N/X_N) \\ FPY &= FPY0 + \Delta_s^{-1}(Z_N/X_N) \end{aligned} \tag{47}$$

where Δ_s is a pixel size in radians per focal plane pixel. These coordinates give the angle at which the photon emerged from the HRMA mirror. We select a nominal pixel size of 0.1 arcseconds. Note that these pixels are not the same size as the detector pixels; the size in mm of these pixels at the physical focus is

$$\Delta_{ps} = f\Delta_s \tag{48}$$

where f is the focal length.

Note that X_N is negative for locations on the detector side of the mirrors, so the FP coordinates now are parallel to decreasing RA and increasing Dec, as we will want for the sky image.

2.4.2 Tangent Plane Pixel Coordinates (TP-1.0)

The Tangent Plane pixel coordinate system plays the role of the system referred to as Boresighted Detector Coordinates in previous missions. It is not really detector coordinates, since it is assumed to lie in the observed tangent plane and so accounts for distorting effects of the mirrors (in the past, we've assumed the detector produces a perfect tangent plane). This system is used to apply calibrations which do not depend on a knowledge of the spacecraft aspect solution. In the case of zero roll angle, TPX is in the direction of decreasing RA and TPY is in the direction of increasing Dec.

Tangent plane coordinates are related to Focal Plane Pixel Coordinates by the application of small corrections to account for mirror effects.

$$\begin{aligned} TPX &= FPX + \Delta FPX(FPX, FPY) \\ TPY &= FPY + \Delta FPY(FPX, FPY) \end{aligned} \tag{49}$$

Table 18: TP and Sky pixel image centers

Instrument	System	TPX0, TPY0	Image size
ACIS	TP, Sky	4096.5,4096.5	8192 x 8192
HRC	TP, Sky	16384.5, 16384.5	32768 x 32768

For ACIS, we choose sky pixel coordinates of exactly 0.5 arcseconds for convenience. This is a 1.5 percent change in pixel size. For HRC, we choose one-eighth-arcsecond pixels so that the HRC pixels are exactly a factor of four smaller than the ACIS ones. This is a 5 percent change in the HRC pixel size compared to detector pixels.

Table 19: Pixel Sizes (assuming flight focal length)

Instrument	System	Size at Focal Plane Δ_p, Δ_{ps} (mm)	Angular Size Δ_s (arcsec)
ACIS	Detector	0.024004	0.492
HRC	Detector	0.006430	0.132
ACIS	Sky	0.02440	0.500
HRC	Sky	0.00610	0.125

2.4.3 Sky Pixel Coordinates (TP-2.0)

The Sky Pixel coordinate system is a translation and rotation of the Tangent Plane pixel coordinate system to align the image with a nominal pointing direction and spacecraft roll angle. For small aspect corrections, sky pixel coordinates are

$$\begin{aligned} X &= X0 + (TPX - TPX0)\cos\gamma - (TPY - TPY0)\sin\gamma + A_X \\ Y &= Y0 + (TPX - TPX0)\sin\gamma + (TPY - TPY0)\cos\gamma + A_Y \end{aligned} \tag{50}$$

where we usually choose $X0 = TPX0, Y0 = TPY0$. The quantities A_X and A_Y are the sky frame aspect offsets in pixels, determining the sky pixel coordinates of the optical axis. (Note that the aspect offsets for Einstein and Rosat were stored as detector frame offsets, which required applying the roll angle to; it's not clear to me why this choice was made.)

In general when combining data over a wide range of pointing directions, (mosaicing images) we must reproject to the nominal sky tangent plane.

2.4.4 Physical Tangent Plane coordinates (PTP-1.0)

If the Tangent Plane pixel coordinates represent a position on the tangent plane to the unit sphere at the optical axis, the Physical Tangent Plane coordinate system

$$\begin{pmatrix} X_{PTP} \\ Y_{PTP} \\ Z_{PTP} \end{pmatrix} = \begin{pmatrix} -\Delta_s(TPX - TPX0) \\ \Delta_s(TPY - TPY0) \\ 1 \end{pmatrix}. \tag{51}$$

represents the 3D vector from the center of the unit sphere to that position on the tangent plane, which the convention that the X_{PTP} and Y_{PTP} axes run in the direction of increasing RA and Dec respectively in the on-orbit case with zero roll.

2.4.5 Physical Sky Plane coordinates (PSP-1.0)

The Physical Sky Plane coordinate system for zero aspect offset and finite roll angle is

$$\begin{pmatrix} X_{PSP} \\ Y_{PSP} \\ Z_{PSP} \end{pmatrix} = \begin{pmatrix} X_{PTP}\cos\gamma + Y_{PTP}\sin\gamma \\ X_{PTP}\sin\gamma - Y_{PTP}\cos\gamma \\ Z_{PTP} \end{pmatrix} \tag{52}$$

where γ is the spacecraft roll angle. The full expression is given in the appendix.

The PTP and PSP systems are important as you need them to calculate the RA and Dec.

2.5 Angular coordinate systems

These systems are used as world coordinate systems applied to the tangent plane and sky pixel systems.

2.5.1 J2000 Celestial Coordinates

One can go from Tangent Plane Physical coordinates to J2000 celestial coordinates using the instantaneous pointing direction (α_A, δ_A). and roll angle γ_A.

$$\mathcal{S}(\alpha,\delta) = \mathrm{Rot}(\pi/2 + \gamma_A, \pi/2 - \delta_A, \pi - \alpha_A) \begin{pmatrix} X_{PTP} \\ Y_{PTP} \\ Z_{PTP} \end{pmatrix} \tag{53}$$

Use the nominal pointing direction (α_0, δ_0) and set the roll angle to zero if using Sky Plane Physical Coordinates:

$$\mathcal{S}(\alpha,\delta) = \mathrm{Rot}(\pi/2, \pi/2 - \delta_0, \pi - \alpha_0) \begin{pmatrix} X_{PSP} \\ Y_{PSP} \\ Z_{PSP} \end{pmatrix} \tag{54}$$

From TP pixel coordinates, recall that

$$\begin{pmatrix} X_{PTP} \\ Y_{PTP} \\ Z_{PTP} \end{pmatrix} = \begin{pmatrix} -\Delta_s(TPX - TPX0) \\ \Delta_s(TPY - TPY0) \\ 1 \end{pmatrix} \tag{55}$$

2.5.2 HRMA Left Handed Spherical Coordinates (HSC-1.1)

This system is used to express off-axis angles. We define HRMA Spherical Coordinates (r, θ_H, ϕ_H) in terms of HRMA nodal Cartesian coordinates as follows:

$$\begin{pmatrix} X_N \\ Y_N \\ Z_N \end{pmatrix} = \begin{pmatrix} +rcos\theta_H \\ -r\sin\theta_H\cos\phi_H \\ r\sin\theta_H\sin\phi_H \end{pmatrix} \tag{56}$$

The inverse is

$$\begin{aligned} r &= \sqrt{X_N^2 + Y_N^2 + Z_N^2} \\ \theta_H &= \cos^{-1}(X_N/r) \\ \phi_H &= \arg(-Y_N, Z_N) \end{aligned} \tag{57}$$

This coordinate system is used for input to the XRCF Test Database; it is a LEFT HANDED coordinate system. The XRCF test database immediately converts these to pitch and yaw. The north pole of this system is the center of the forward aperture of the HRMA A0; θ_H measures the off-axis angle of the incoming ray and ϕ_H measures its azimuth in the Y_N, Z_N plane such that for an observer at XRCF standing by the SI and looking at the XSS, $\phi_H = 0$ is to the left and $\phi_H = \pi/2$ is vertically downwards.

Then the forward aperture of the HRMA, A0, has HRMA nodal coordinates $(a, 0, 0)$ and HSC coordinates $(a, 0, 0)$. The focal point F of the HRMA has HRMA nodal coordinates $(-f, 0, 0)$ and HSC coordinates $(f, \pi, 0)$.

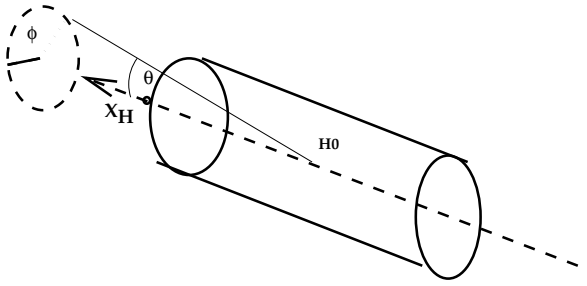

Figure 18: HRMA spherical coordinates

2.5.3 HRMA Right Handed Spherical Coordinates (HSC-1.2)

To satisfy my desire for using left handed systems as little as possible, I define HSC-1.2 to be the same as HSC-1.1 except that the azimuth increases in the opposite direction: $\phi_{HR} = 0$ is to the left and $\phi_{HR} = \pi/2$ is vertically upwards.

$$\begin{pmatrix} X_N \\ Y_N \\ Z_N \end{pmatrix} = \begin{pmatrix} rcos\theta_{HR} \\ -r\sin\theta_H\cos\phi_H \\ -r\sin\theta_H\sin\phi_H \end{pmatrix} \tag{58}$$

The inverse is

$$\begin{aligned} r &= \sqrt{X_N^2 + Y_N^2 + Z_N^2} \\ \theta_{HR} &= \cos^{-1}(X_N/r) = \theta_H \\ \phi_{HR} &= \arg(-Y_N, -Z_N) = -\phi_H \end{aligned} \tag{59}$$

2.5.4 HRMA rotation coordinates (Pitch and Yaw) (HSC-3.0)

A third choice of pole is the $+Y_N$ axis, whose latitude-like coordinates α_z is called **yaw**, and whose azimuthal coordinate α_y is called **pitch**. The mapping between pitch and yaw coordinates and HRMA coordinates is

$$\begin{pmatrix} X_N \\ Y_N \\ Z_N \end{pmatrix} = \begin{pmatrix} +r\cos\alpha_z\cos\alpha_y \\ +r\sin\alpha_z \\ -r\cos\alpha_z\sin\alpha_y \end{pmatrix} \tag{60}$$

or

$$\begin{aligned} \alpha_z &= \sin^{-1}(Y_N/R) \\ \alpha_y &= \arg(X_N, -Z_N) \end{aligned} \tag{61}$$

The rotation matrix from HSC-1.2 right-handed spherical coords is

$$\mathrm{R(HSC\text{-}1.2,HSC\text{-}3.0)} = \mathrm{Rot}(\pi, \pi/2, \pi). \tag{62}$$

The motivation for this coordinate system is its relationship to the commanded pitch and yaw of the HRMA at XRCF. We call the pitch and yaw coordinates of the XSS $\alpha_y(XSS) = \alpha_{y0}$ and $\alpha_z(XSS) = \alpha_{z0}$. To put the XSS at these coordinates, the HRMA must be yawed α_{z0} to the left and its aperture pitched α_{y0} downward.

2.5.5 HRMA Source coordinates (HSC-2.1)

The HRMA Source Coordinate system (r, az, el) is a pseudo RA, Dec system that gives the 'sky' position of the source as seen by the HRMA. Unlike HRMA spherical coordinates, they have a

pole at $-Z_N$ rather than X_N. The relationship between Source coordinates and HRMA nodal coordinates is:

$$\begin{pmatrix} X_N \\ Y_N \\ Z_N \end{pmatrix} = \begin{pmatrix} +r\cos\mathrm{el}\cos\mathrm{az} \\ -r\cos\mathrm{el}\sin\mathrm{az} \\ -r\sin\mathrm{el} \end{pmatrix} \tag{63}$$

Coordinates az =0, el = 0 refer to a source on the HRMA axis (center of the field of view); positive el gives a source above the HRMA axis (top of the field of view), while positive az gives a source to the left of the center of the field of view. (HSC-2.0 had az going the other way, creating a left-hand system). The inverse function is

$$\begin{aligned} \mathrm{el} &= \sin^{-1}(-Z_N/r) \\ \mathrm{az} &= \arg(X_N, -Y_N) \end{aligned} \tag{64}$$

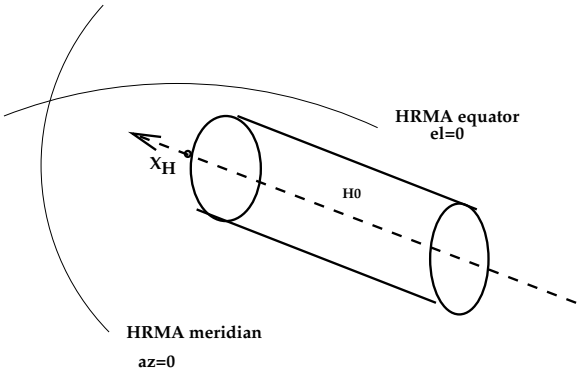

Figure 19: HRMA source coordinates

The rotation matrices from the other HRMA angular systems are

$$\mathrm{R(HSC\text{-}1.2,HSC\text{-}2.1)} = \mathrm{Rot}(\pi/2, \pi/2, \pi); \quad \mathrm{R(HSC\text{-}3.0,HSC\text{-}2.1)} = \mathrm{Rot}(\pi/2, \pi/2, 3\pi/2). \tag{65}$$

2.6 Grating data

When we observe with the gratings, we get a dispersed spectrum with orders +1, -1, +2, -2, ... and a zero-order undispersed image. The undispersed (zero-order) photons do not interact with the gratings and we can deal with them using the same analysis as for imaging detectors. To analyse a dispersed photon, however, we must know the location of the zero-order image as well as that of the dispersed photon. For instance, spacecraft roll aspect must be applied to the zero-order position, not the dispersed position.

The location of the zero order photon must be calculated relative to the Grating Node rather than the HRMA Node. The Grating Node is on the optical axis at a distance R from the focus,

where R is the diameter of the Rowland Circle. The nominal Rowland Circle diameter is quoted as 8650.0 mm [1], Appendix A, p. 11; 8633.69 mm [1], Drawing 301331, Sheet 3; and 8636.00 mm [3]. I will adopt the value from the drawing, i.e. 8633.69mm. (However View F on the same drawing shows the Rowland circle intercepting the X axis at $X_A = 372.116$ corresponding to R = 8643.11 mm. This is an error caused by confusing H0 and H1 when measuring the location of the OTG origin.)

2.6.1 Grating Nodal Coordinates (OTG-1.0)

The HNC coordinates of the Grating Node $\boldsymbol{G0}$ in flight are

$$\begin{pmatrix} X_N(G0) \\ Y_N(G0) \\ Z_N(G0) \end{pmatrix} = \begin{pmatrix} -1431.81 \\ 0 \\ 0 \end{pmatrix} \tag{66}$$

The exact value is different at XRCF.

In general, we define Grating Nodal Coordinates GNC as

$$\begin{pmatrix} X_{GN} \\ Y_{GN} \\ Z_{GN} \end{pmatrix} = \begin{pmatrix} X_N \\ Y_N \\ Z_N \end{pmatrix} - \begin{pmatrix} X_N(G0) \\ Y_N(G0) \\ Z_N(G0) \end{pmatrix} \tag{67}$$

These are the same as the project OTG coordinates, except that their origin is at the grating node and not at the OTG surface:

$$(X_{GN}, Y_{GN}, Z_{GN}) = (X_G, Y_G, Z_G) - \begin{pmatrix} 63.500 \\ 0 \\ 0 \end{pmatrix} \tag{68}$$

2.6.2 Grating Zero Order Coordinates (GZO-1.0)

Next we pick a source, with zero order position $\boldsymbol{ZO}$. and let the vector from the grating node to the source zero order be $\boldsymbol{S}$. Then define

$$\begin{aligned} \boldsymbol{e}_{X_{ZO}} &= -\boldsymbol{S}/|\boldsymbol{S}| \\ \boldsymbol{e}_{Y_{ZO}} &= \boldsymbol{d_0} \wedge \boldsymbol{e}_{X_{ZO}}/|\boldsymbol{d_0} \wedge \boldsymbol{e}_{X_{ZO}}| \\ \boldsymbol{e}_{Z_{ZO}} &= \boldsymbol{e}_{X_{ZO}} \wedge \boldsymbol{e}_{Y_{ZO}} \end{aligned} \tag{69}$$

where the Grating Pole (cross-dispersion unit vector) $\boldsymbol{d_0}$ is

$$\boldsymbol{d_0} = (0, -\sin\alpha_G, \cos\alpha_G) \tag{70}$$

in HNC coordinates, where α_G is the angle between the dispersion direction and the spacecraft Y axis.

This defines a cartesian orthonormal set, Grating Zero Order Coordinates, whose origin we choose to be at $\boldsymbol{G0}$. Diffracted photons travel in the X_{ZO}, Y_{ZO} plane, and the intersection of this plane with the detector surface defines the dispersion direction. For an on-axis source and a grating with $\alpha_G = 0$, Zero Order coordinates are the same as Grating Nodal coordinates.

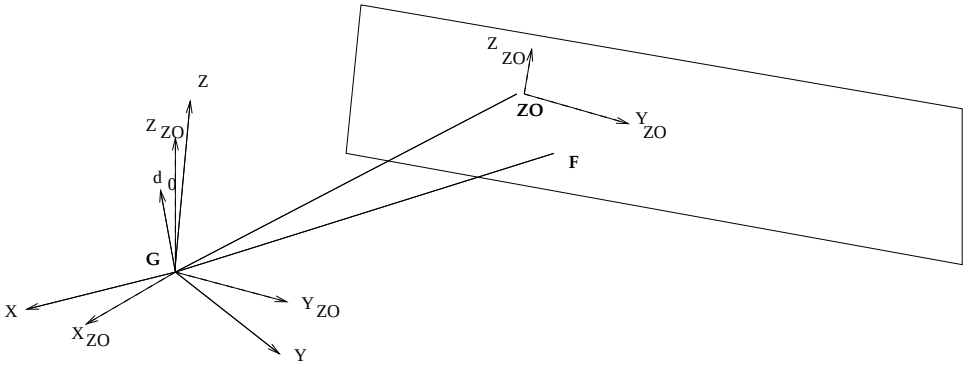

Figure 20: Grating Zero Order coordinates

2.6.3 Grating Diffraction Coordinates (GDC-1.0)

The Grating Diffraction Coordinate system (r_{TG}, d_{TG}) gives the distance in mm along the dispersion direction and in the cross-dispersion direction. We measure the longitude θ_R and latitude θ_D of the diffracted photon in the ZO system,

$$\begin{aligned} r_{TG} &= X_R \theta_R = X_R \tan^{-1}(-Y_{ZO}/X_{ZO}) \\ d_{TG} &= X_R \tan\theta_d = X_R \frac{Z_{ZO}}{\sqrt{X_{ZO}^2 + Y_{ZO}^2}} \sim X_R (Z_{ZO}/X_{ZO}) \end{aligned} \tag{71}$$

Here X_R is the length from the grating node to the focus, which is approximately equal to the length $|\boldsymbol{S}|$.

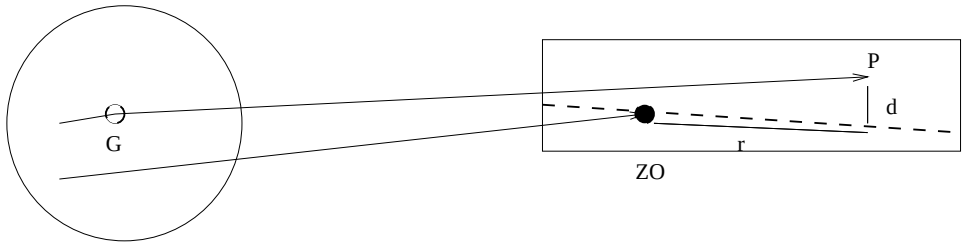

Figure 21: Grating Diffraction coordinates

2.6.4 Grating Diffraction Plane Pixel Coordinates (GDP-1.0)

The Grating Diffraction Plane Pixel Coordinates GDX, GDY are defined by

$$\begin{aligned} GDX &= GDX0 - \Delta_{gs}^{-1}(Y_{ZO}/X_{ZO}) \\ GDY &= GDY0 + \Delta_{gs}^{-1}(Z_{ZO}/X_{ZO}) \end{aligned} \tag{72}$$

analogously to the Focal Plane Pixel Coordinates.

They are related to the physical Grating Diffraction Coordinates by

$$\begin{aligned} GDX &= GDX0 + \Delta_{gs}^{-1}\tan(r_{TG}/X_R) \\ GDY &= GDY0 + \Delta_{gs}^{-1}(d_{TG}/X_R)\cos(r_{TG}/X_R) \end{aligned} \tag{73}$$

Now the LETG is normally used with HRC and the HETG with ACIS. Note that the GDC are centered at the zero order position for the source, which in principle can be a long way off axis. The coordinate parameters for the gratings are listed below. We use the same physical pixel size as for the detector systems, which correspond to somewhat different angular sizes than the imaging case because we are measuring angles from G rather than H0.

Table 20: GDC pixel image centers

Instrument	System	GDX0, GDY0	Image size
ACIS	GDC	4096.5, 4096.5	8192 x 8192
HRC	GDC	32768.5, 32768.5	65536 x 65536

Table 21: GDP Pixel Sizes (assuming flight Rowland radius)

Instrument	System	Size at Focal Plane Δ_p, Δ_{gp} (mm)	Angular Size $\Delta_g s$ (arcsec)
ACIS	Detector	0.024004	0.573
HRC	Detector	0.006430	0.154

2.6.5 Dispersion relation

The wavelength of the diffracted photon is

$$\lambda = P\sin\theta_R/m \tag{74}$$

where P is the average grating period and m is the diffraction order. So

$$\lambda \sim (P/m)(GDX - GDX0)\Delta_{gs} \tag{75}$$

The average grating periods for the three gratings are given in the table below.

Table 22: Grating properties

Instrument	P	α_G (deg)
HETG	2000.0$\AA$	5.0
METG	4000.0$\AA$	-5.0
LETG	9921.0$\AA$	+0.0

3 XRCF Data Analysis

3.1 XRCF coordinate systems

3.1.1 HRMA coordinates (HRMA-2.0) at XRCF

Since the HRMA is mounted upside down at XRCF, the positive Z_H axis is along the local DOWNWARD vertical when HRMA is in its default configuration in the XRCF.

In the XRCF default configuration

$$\begin{pmatrix} X_H \\ Y_H \\ Z_H \end{pmatrix} = \begin{pmatrix} +X_{XRCF} \\ -Y_{XRCF} \\ -Z_{XRCF} \end{pmatrix} \tag{76}$$

3.1.2 XRCF facility coordinates (XRCF-1.0)

The XRCF Facility coordinate system $(X_{XRCF}, Y_{XRCF}, Z_{XRCF})$ ('XRCF coords') has its origin at the HRMA CAP midplane X0, which is close to the center point H0 (the point about which the HRMA is rotated at the XRCF). The X-axis is the Facility Optical Axis, and the Z-axis is the local vertical. Units of XRCF coordinates shall be mm.

The SI default reference point $\boldsymbol{S}$ is located at the HRMA on-facility-axis focus $\boldsymbol{F0}$, at XRCF coords $(-f, 0, 0)$ where we currently believe f = 10258.3. The value may change.

3.1.3 DFC coordinates (XRCF-2.0)

The Default FAM coordinates (DFC) are the coordinate system (frame F3 in Ball's notation) in which the movement of the FAM feet relative to their boresight positions is measured. More importantly for data analysis, they are the coordinate system in which the FAM data records record the (X,Y,Z) and $(\theta_X, \theta_Y, \theta_Z)$ of the FAM.

The FAM axes in the default, boresight configuration (DFC coordinates) are nominally parallel to the XRCF axes but there may be some misalignment. We encode this misalignment in the FAM

Frame Euler Angles $\phi_{EF}, \theta_{EF}, \psi_{EF}$ of the rotation matrix R(XRCF,DFC) whose default values are $Rot(0,0,0)$ (TBR after installation). Since the DFC coordinates are fixed with respect to the XRCF, we give them the identifier XRCF-2.0. The origin of DFC coordinates is taken to be F0, the HRMA focus in the default configuration.

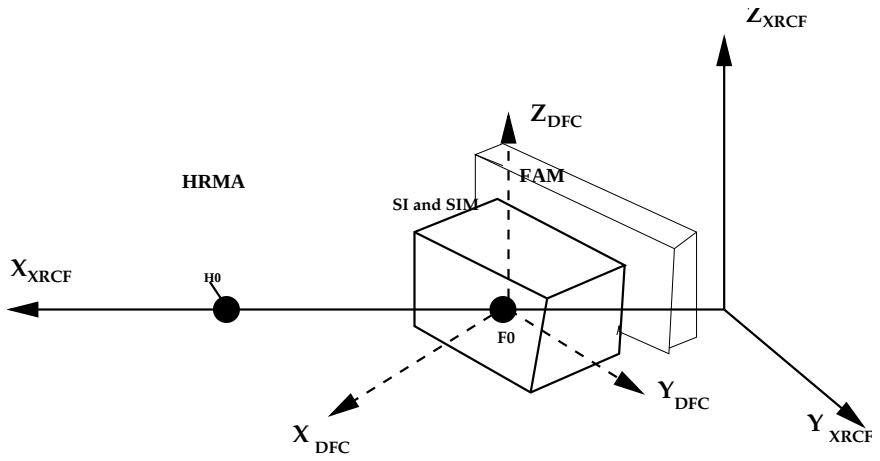

Figure 22: XRCF Coordinates and DFC Coordinates. The DFC coordinates give the misalignment of the FAM in its default position. The misalignment is highly exaggerated in the diagram.

3.1.4 FAM coordinates (FAM-1.0)

In the default, boresight configuration the FAM axes are intended to be parallel to the XRCF (and LSI) axes, but there may be some misalignment. The FAM encoders measure the movement of the FAM relative to its boresight position, not relative to the XRCF. Therefore, we need to describe the motion of the FAM by defining two new coordinate systems, one fixed in the FAM (FAM coordinates) and one fixed in the XRCF but with axes aligned with the FAM default position (DFC coordinates). At the boresight position, DFC and FAM (Ball frame F5) coordinates are coincident.

Specifically, we define FAM coordinates (X_F, Y_F, Z_F) to be fixed in the FAM, with the X axis normal to the payload interface plane and the Y, Z axes in that plane and specified by the alignment cubes on the FAM. The center of the FAM aperture is at FAM coordinates $(c_1, 0.0, 0.0)$ where $c_1 = 77.47$ if the units of the system are chosen to be mm. DFC coordinates are then defined to coincide with FAM coordinates when the FAM readouts are all zero. (Note: In the Ball SER memo, DFC is frame F3, FAM is fram F5, and LSI is frame F7).

3.1.5 XRCF SI Installation Coordinates (STF-2.0)

SI Installation Coordinates (SIC) are an intermediate system used in correcting for dither. They describe the orientation of the STF (LASSZ) frame with respect to the XRCF when the FAM is at

its home position, but are considered to be fixed with respect to the FAM/LASSZ. They share the same origin as STF coordinates:

$$P(SIC) = R(STF, SIC)P(STF) = Rot(3\pi/2, \pi + \psi_r, \pi/2) \tag{77}$$

and the rotation matrix is the product of the instrument roll misalignment $Rot(3\pi/2, \psi_r, \pi/2)$ and the fact that the STF is upside down with respect to the XRCF, $Rot(3\pi/2, \pi, \pi/2)$.

3.2 XRCF coordinate transformations

3.2.1 Specifying the HRMA orientation in the XRCF

In the default configuration C0, HRMA coordinates are identical to XRCF coordinates. However, the HRMA can change its pitch and yaw. I adopt the Ball notation, in which the **HRMA Yaw (Azimuth)** α_z is positive if the aperture of the HRMA is moved to the left of the FOA (as seen by someone standing at the SIs, i.e. the XRCF Y_{XRCF}-coordinate of A0 is positive), and the **HRMA Pitch (Elevation)** α_y is positive if the aperture of the HRMA is moved downward (so that the elevation of the XSS relative to the HRMA centerline increases, and the XRCF Z_{XRCF}-coordinate of A0 is negative).

The XRCF test database stores the HRMA pitch and yaw, but is created using inputs of the HRMA polar angle and polar azimuth (ζ_p, ζ_a). These are the HRMA spherical coordinates of the XSS.

The polar angle is the angle between X_N and X_{XRCF}, while the polar azimuth is the angle between Y_N and $-Y_{XRCF}$ in the Y_{XRCF}, Z_{XRCF} plane. These angles are directly related to the HRMA spherical coordinates of the XSS. If the XSS is at HSC (r, θ, ϕ) then the HRMA polar angles are $\zeta_p = \theta$, $\zeta_a = \phi$. The test database angles and the mechanically commanded angles are related by

$$\begin{aligned} \cos\alpha_z \cos\alpha_y &= \cos\zeta_p \\ \sin\alpha_z &= -\sin\zeta_p \cos\zeta_a \\ \cos\alpha_z \sin\alpha_y &= -\sin\zeta_p \sin\zeta_a \end{aligned} \tag{78}$$

So for example, if the test database commands an off axis angle of ζ_p=0.5 arcmins and a polar azimuth of ζ_a=90 degrees, the required pitch and yaw are α_y=-0.5 arcmins, α_z=0, and the nose of the HRMA is raised by 0.5 arcmin. If the polar azimuth is instead 45 degrees, we have α_y=-0.35 arcmins, α_z=-0.35 arcmins, and the HRMA is raised by 0.35 arcmins and yawed by 0.35 arcmins to the right; conversely, the image of the XSS in the HRMA focal plane moves down and to the left.

3.2.2 XRCF to HNC transformation

In terms of the pitch and yaw, the transformation between XRCF and HNC coordinates is given by the translation vector $H0(N) = (X_N(H1), 0, 0)$ and the Euler rotation matrix

$$R(X, N) = Rot(\alpha_z, \pi + \alpha_y, \pi) \tag{79}$$

or explicitly

$$\begin{aligned} X_N &= (X_{XRCF} - X_{XRCF}(H0)) \cos\alpha_z \cos\alpha_y + Y_{XRCF} \sin\alpha_z \cos\alpha_y - Z_{XRCF} \sin\alpha_y \\ Y_N &= (X_{XRCF} - X_{XRCF}(H0)) \sin\alpha_z - Y_{XRCF} \cos\alpha_z \\ Z_N &= -(X_{XRCF} - X_{XRCF}(H0)) \cos\alpha_z \sin\alpha_y - Y_{XRCF} \sin\alpha_z \sin\alpha_y - Z_{XRCF} \cos\alpha_y \end{aligned} \tag{80}$$

and the inverse

$$\begin{aligned} X_{XRCF} &= X_{XRCF}(H0) + X_N \cos\alpha_z \cos\alpha_y + Y_N \sin\alpha_z - Z_N \cos\alpha_z \sin\alpha_y \\ Y_{XRCF} &= X_N \sin\alpha_z \cos\alpha_y - Y_N \cos\alpha_z - Z_N \sin\alpha_z \sin\alpha_y \\ Z_{XRCF} &= -X_N \sin\alpha_y - Z_N \cos\alpha_y \end{aligned} \tag{81}$$

Note that for zero pitch and yaw,

$$\begin{aligned} X_N &= (X_{XRCF} - X_{XRCF}(H0)) \\ Y_N &= -Y_{XRCF} \\ Z_N &= -Z_{XRCF} \end{aligned} \tag{82}$$

reflecting the fact that the mirror is installed upside down at the XRCF.

So in particular if the focal point $P_N(F) = (-f, 0, 0)$ then

$$P_{XRCF}(F) = (X_{XRCF}(H0) - f\cos\alpha_z \cos\alpha_y, -f \sin\alpha_z \cos\alpha_y, f \sin\alpha_y) \tag{83}$$

For some reason the Ball SER approximates this as

$$P_X(F) \sim (-f \cos\sqrt{(}\alpha_z^2 + \alpha_y^2), -f \sin\alpha_z, f \sin\alpha_y) \tag{84}$$

which is OK for small α_y,α_z.

The XSS is at HRMA nodal coordinates

$$\begin{pmatrix} X_N(XSS) \\ Y_N(XSS) \\ Z_N(XSS) \end{pmatrix} = \begin{pmatrix} +LS\cos\alpha_z \cos\alpha_y \\ +LS\sin\alpha_z \\ -LS\cos\alpha_z \sin\alpha_y) \end{pmatrix} \tag{85}$$

3.2.3 DFP coordinates (FP-2.0)

At the XRCF:

$$\begin{pmatrix} X_{STF} \\ Y_{STF} \\ Z_{STF} \end{pmatrix} = \begin{pmatrix} X_{STF}(\Sigma) \\ Y_{STF}(\Sigma) \\ Z_{STF}(\Sigma) \end{pmatrix} + R(N, STF) \begin{pmatrix} X_N - f \\ Y_N \\ Z_N \end{pmatrix} \tag{86}$$

where R(N, STF) is a rotation matrix which depends on the orientation of the FAM. In the nominal (aligned) configuration $P_{STF}(\Sigma) = \mathbf{0}$ and $R(N, STF) = 1$ so that

$$\begin{pmatrix} X_{STF} \\ Y_{STF} \\ Z_{STF} \end{pmatrix} = \begin{pmatrix} X_N - f \\ Y_N \\ Z_N \end{pmatrix} \tag{87}$$

We define Dithered Focal Plane pixel coordinates by

$$\begin{aligned} DFPX &= FPX0 - \Delta_s(Y_{STF}/(X_{STF} + f) \\ DFPY &= FPY0 + \Delta_s(Z_{STF}/X_{STF} + f) \end{aligned} \tag{88}$$

so that in flight, or at XRCF with no dither or offset, DFP and FP coordinates are identical. At XRCF, they differ due to dither. This allows us to inspect the effects of dither independently of any other effects.

3.3 XRCF forward coordinate thread

The XRCF forward coordinate thread illustrates the prediction of the detector position of the center of the X-ray beam for a particular XRCF observation.

- Step 1: Obtain the HRMA spherical coordinates of the XSS. The test database parameters HRMA polar angle hrma_pol and HRMA azimuth hrma_az are exactly the HRMA spherical coordinates hrma_pol = $\theta_H(XSS)$, hrma_az = $\phi_H(XSS)$ of the X-ray source.
- Step 2: Convert these to the commanded pitch and yaw of the XSS.

$$\begin{aligned} \alpha_z(XSS) &= \sin^{-1}\left(-\sin(\theta_H(XSS))\cos(\phi_H(XSS))\right) \\ \alpha_y(XSS) &= \sin^{-1}\left(-\sin(\theta_H(XSS))\sin(\phi_H(XSS))\sec(\alpha_z(XSS))\right) \end{aligned} \tag{89}$$

- Step 3: Convert the incoming photon az and el or pitch and yaw to Tangent Plane pixel coordinates.
- Step 4: Correct the Tangent Plane coordinates to Focal Plane coordinates.
- Step 5: Convert Focal Plane coordinates to a HRMA Nodal Coordinate vector.

- Step 6: Convert the nodal coordinates of the HRMA node and of the ray direction to LSI coordinates for the current detector. This involves computing the LSI to HNC transformation, which depends on the current FAM and LASSZ positions.
- Step 6: Calculate the intersection of the ray with each of the detector chip planes, giving a chip ID and the CPC coordinates of the intersection.
- Step 7: Convert the CPC coordinates to chip and detector coordinates.

3.4 XRCF backward coordinate thread

The calculation going from CHIP to TDET and/or STF coordinates is unchanged; we treat the LASSZ device as if it were identical to the SIM, although it is possible that slightly different STT coordinates for the detectors will be needed. Similarly, the process of going from HNC coordinates to FP pixels to TP pixels is unchanged, although because of the 1G effects it is possible that the $\Delta FPX, \Delta FPY$ functions may be slightly different. However, going from STF to HNC coordinates is more complicated.

First, I describe the full STF to HNC transformation; in a later rev I will describe the same transformation in terms of an offset from a nominal value.

3.4.1 STF to FAM coordinates

The STF (LASSZ) and FAM frames share the same origin but the axes are misaligned:

$$P(FAM) = R(STF, FAM)P(STF) = R(XRCF, DFC)R(STF, SIC)P(STF) \tag{90}$$

The rotation matrix is the product of the DFC to XRCF misalignment matrix and the SI installation matrix, since when the FAM is in the home position the SIC and XRCF axes should line up.

3.4.2 FAM to DFC coordinates

The FAM feet are moved so that the FAM/STF origin Σ is displaced and the orientation of the FAM is changed:

$$P(DFC) = \Sigma(DFC) + R(FAM, DFC)P(FAM) \tag{91}$$

where

$$R(FAM, DFC) = Rot(3\pi/2, \theta_X, \pi/2)Rot(\theta_Y, \theta_Z, 0) \tag{92}$$

and

$$\Sigma(DFC) = \begin{pmatrix} X \\ Y \\ Z \end{pmatrix}. \tag{93}$$

Here the values of (X,Y,Z) and $(\theta_X, \theta_Y, \theta_Z)$ are obtained from the FAM data records.

3.4.3 DFC to XRCF coordinates

Now we reapply the misalignment matrix to get the position of the pixel in XRCF coordinates:

$$P(XRCF) = \Sigma_0(XRCF) + R(DFC, XRCF)P(DFC) \tag{94}$$

3.4.4 XRCF to HRMA nodal coordinates

To go to HNC coordinates, we apply the HRMA pitch and yaw:

$$P(HNC) = R(XRCF, HNC)(P(XRCF) - N(XRCF)) \tag{95}$$

Thus the complete STF to HNC transformation is

$$P(HNC) = \Sigma(HNC) + R(STF, HNC)P(STF) \tag{96}$$

where

$$\Sigma(HNC) = R(XRCF, HNC)(\Sigma_0(XRCF) - N(XRCF) + R(DFC, XRCF)\Sigma(DFC)) \tag{97}$$

and

$$R(STF, HNC) = R(XRCF, HNC)R(DFC, XRCF)R(FAM, DFC)R(XRCF, DFC)R(STF, SIC). \tag{98}$$

3.4.5 Case of on-axis source and no dither

In the case where there is no dither offset and no HRMA tilt, $\Sigma(DFC) = 0$ and R(FAM,DFC)=1, while R(XRCF,HNC)=Rot$(3\pi/2, \pi, \pi/2)$. Then

$$R(XRCF, STF) = Rot(3\pi/2, \psi_r + \pi, \pi/2) \tag{99}$$

and

$$\begin{pmatrix} X_{STF} \\ Y_{STF} \\ Z_{STF} \end{pmatrix} = \begin{pmatrix} X_{XRCF} + f \\ -Y_{XRCF}\cos\psi_r - Z_{XRCF}\sin\psi_r \\ Y_{XRCF}\sin\psi_r - Z_{XRCF}\cos\psi_r \end{pmatrix} \tag{100}$$

and

$$\begin{pmatrix} X_{STF} \\ Y_{STF} \\ Z_{STF} \end{pmatrix} = \begin{pmatrix} X_N + f \\ Y_N\cos\psi_r + Z_N\sin\psi_r \\ -Y_N\sin\psi_r + Z_N\cos\psi_r \end{pmatrix} \tag{101}$$

3.4.6 Case of tilted HRMA with no dither

In the **nominal configuration** CN, the SIM is moved so that the X_{STF} axis is coincident with the HRMA axis X_N. Then R(HNC,STF) = Rot$(3\pi/2, \psi_r, \pi/2)$, so

$$\begin{pmatrix} X_{STF} \\ Y_{STF} \\ Z_{STF} \end{pmatrix} = \begin{pmatrix} f \\ 0 \\ 0 \end{pmatrix} + \begin{pmatrix} X_N \\ Y_N \cos\psi_r + Z_N \sin\psi_r \\ -Y_N \sin\psi_r + Z_N \cos\psi_r \end{pmatrix} \tag{102}$$

and,

$$\begin{aligned} \begin{pmatrix} X_{STF} \\ Y_{STF} \\ Z_{STF} \end{pmatrix} &= \begin{pmatrix} f \\ 0 \\ 0 \end{pmatrix} + X_{XRCF} \begin{pmatrix} \cos\alpha_z \cos\alpha_y \\ -\sin\psi_r \cos\alpha_z \sin\alpha_y + \cos\psi_r \sin\alpha_z \\ -\sin\psi_r \sin\alpha_z - \cos\psi_r \cos\alpha_z \sin\alpha_y \end{pmatrix} \\ &+ Y_{XRCF} \begin{pmatrix} \sin\alpha_z \cos\alpha_y \\ -\cos\psi_r \cos\alpha_z - \sin\psi_r \sin\alpha_z \sin\alpha_y \\ -\cos\psi_r \sin\alpha_z \sin\alpha_y + \sin\psi_r \cos\alpha_z \end{pmatrix} \\ &+ Z_{XRCF} \begin{pmatrix} -\sin\alpha_y \\ -\sin\psi_r \cos\alpha_y \\ -\cos\psi_r \cos\alpha_y \end{pmatrix} \end{aligned} \tag{103}$$

The inverse transformations are:

$$\begin{aligned} \begin{pmatrix} X_{XRCF} \\ Y_{XRCF} \\ Z_{XRCF} \end{pmatrix} &= (X_{STF} - f) \begin{pmatrix} \cos\alpha_z \cos\alpha_y \\ -\sin\alpha_z \cos\alpha_y \\ \sin\alpha_y \end{pmatrix} \\ &+ Y_{STF} \begin{pmatrix} \sin\psi_r \cos\alpha_z \sin\alpha_y - \cos\psi_r \sin\alpha_z \\ -\cos\psi_r \cos\alpha_z - \sin\psi_r \sin\alpha_z \sin\alpha_y \\ -\cos\alpha_y \sin\psi_r \end{pmatrix} \\ &+ Z_{STF} \begin{pmatrix} \cos\psi_r \cos\alpha_z \sin\alpha_y + \sin\psi_r \sin\alpha_z \\ -\cos\psi_r \sin\alpha_z \sin\alpha_y + \sin\psi_r \cos\alpha_z \\ -\cos\alpha_y \cos\psi_r \end{pmatrix} \end{aligned} \tag{104}$$

and

$$\begin{aligned} X_N &= X_{STF} - f \\ Y_N &= Y_{STF} \cos\psi_r - Z_{STF} \sin\psi_r \\ Z_N &= Z_{STF} \cos\psi_r + Y_{STF} \sin\psi_r \end{aligned} \tag{105}$$

The rotation of the SI about the Z_{XRCF} axis is $\psi 1_z = \alpha_z$, about the Y_{XRCF} axis is $\psi 1_y = \alpha_y$, and about the X_{XRCF} axis is $\psi 1_x = \psi_r$ (Ball SER). We now reproduce the transformation matrix

in the SER eq.5a,

$$R(XRCF,STF) \sim \begin{bmatrix} 1 & +\psi 1_z & -\psi 1_y \\ (\psi_1 x \psi 1_y - \psi_1 z) & +(1+\psi 1_x \psi 1_z \psi 1_y) & +(\psi 1_x) \\ (\psi 1_x \psi 1_z + \psi 1_y) & +(\psi 1_z \psi 1_y - \psi_1 x) & +1 \end{bmatrix} \tag{106}$$

which follows easily from setting $\cos X = 1, \sin X = X$ in R(XRCF,STF).

3.4.7 STF to HRMA coordinates: case with dither or offset

We expect that the SI will always be close to the nominal configuration CN, but with small offsets. Suppose that due to FAM movement the SI origin is offset from the nominal position by (possibly large due to defocus or off axis tests) $\Delta S = (\Delta S1, \Delta S2, \Delta S3)$ and the FAM pitch and yaw are offset by a small $\Delta\alpha_y$, $\Delta\alpha_z$. (we assume the roll offset $\Delta\psi = 0$). We will keep only first order in the pitch and yaw offsets. Then

$$\begin{pmatrix} X_N \\ Y_N \\ Z_N \end{pmatrix} = \begin{pmatrix} -f \\ 0 \\ 0 \end{pmatrix} + (I + \Delta R_z \Delta\alpha_z + \Delta R_y \Delta\alpha_y) \begin{pmatrix} X_{STF} \\ Y_{STF}\cos\psi_r - Z_{STF}\sin\psi_r \\ Y_{STF}\sin\psi_r + Z_{STF}\cos\psi_r \end{pmatrix} + R_{XN}\Delta S \tag{107}$$

where I is the unit matrix and the adjustment matrices ΔR_z and ΔR_y are

$$\Delta R_z = \begin{pmatrix} -\sin\alpha_z\cos\alpha_y & -\cos\alpha_z & -\sin\alpha_z\sin\alpha_y \\ -\sin\alpha_z\sin\alpha_y & -\sin\alpha_z & \cos\alpha_z\sin\alpha_y \\ 0 & 0 & 0 \end{pmatrix} \tag{108}$$

and

$$\Delta R_y = \begin{pmatrix} -\cos\alpha_z\sin\alpha_y & 0 & \cos\alpha_z\cos\alpha_y \\ \cos\alpha_z\cos\alpha_y & 0 & \cos\alpha_y\sin\alpha_z \\ -\cos\alpha_y & 0 & \sin\alpha_y \end{pmatrix} \tag{109}$$

Unfortunately we have the angle offsets in DFC coordinates, not HNC coordinates; I have not yet calculated the correction but it will be small. Having obtained the coefficients of the STF to HRMA transformation, we can trivially convert to the coefficients of the DETX, DETY to X, Y transformation, which are more complicated than the usual aspect offset formalism. The aspect offset formalism ignores changes in the focus both with time and spatially across the detector plane, so the full three dimensional STF to HRMA transformation is needed if you want to study such effects.

4 Listing of Other AXAF Coordinate Systems

4.1 Project Coordinate Systems

There are a plethora of existing coordinate systems in use describing positions relative to the HRMA mirror. They are used in the assembly and alignment of the hardware but they will not be used in

the kind of data analysis I am concentrating on in this memo. They are presented for reference.

4.1.1 Orbiter coordinate system

The Space Shuttle Orbiter coordinate system [1] is used to locate the spacecraft within the Orbiter payload bay during the launch phase. It is measured in inches with the $+X_O$ axis downwards at launch (i.e. toward orbiter aft end), the $+Y_O$ axis to starboard, and the $+Z_O$ axis toward the top side (tail side) of the orbiter (i.e. upwards at landing). During launch, the origin of spacecraft coordinates is at orbiter coordinates

$$\begin{pmatrix} X_O \\ Y_O \\ Z_O \end{pmatrix} = \begin{pmatrix} 596.0 \\ 0.0 \\ 400.0 \end{pmatrix} \tag{110}$$

The relation between Orbiter and Spacecraft coordinates is

$$\begin{pmatrix} X_A \\ Y_A \\ Z_A \end{pmatrix} = \begin{pmatrix} X_O - 596.0 \\ Y_O \\ Z_O - 400.0 \end{pmatrix} \tag{111}$$

4.1.2 Payload coordinate system

The Space Shuttle payload coordinate system [1] is fixed with respect to the payload, probably. It is measured in inches. In the stowed position, payload and Orbiter coordinates are parallel, and related by

$$\begin{pmatrix} X_P \\ Y_P \\ Z_P \end{pmatrix} = \begin{pmatrix} X_O - 596.0 \\ Y_O \\ Z_O - 200.0 \end{pmatrix} = \begin{pmatrix} X_A \\ Y_A \\ Z_A + 200.0 \end{pmatrix} \tag{112}$$

(reference [1].)

4.1.3 The Telescope Ensemble Coordinate System

The document EQ7-002 Rev D, [4] describing the HRMA, defines the Telescope Ensemble Coordinate System (X_T, Y_T, Z_T) with somewhat different axis choice (+Z is the optical axis) and with origin at the focus. Presumably this is the on-orbit, zero-g focus f0, but the document doesn't say. The document IF1-20 OBS/SI ICD [1] defines the Telescope Coordinate System (X_T, Y_T, Z_T) to be identical with spacecraft coordinates.

4.1.4 Optical Bench Assembly system

The OBA system [2] is

$$\begin{pmatrix} X_{OBA} \\ Y_{OBA} \\ Z_{OBA} \end{pmatrix} = \begin{pmatrix} X_{FP} - 28.5 \\ Y_{FP} \\ Z_{FP} \end{pmatrix} = \begin{pmatrix} X_A - 60.336 \\ Y_A \\ Z_A \end{pmatrix} \tag{113}$$

(TRW AXAF I system alignment plan). I won't discuss it further.

4.1.5 OTG Coordinates (OTG-2.0)

The OTG coordinates system (X_G, Y_G, Z_G) has X_G parallel to X_H and Y_G, Z_G parallel to Y_A, Z_A $X_G = 0$ is the side of the OTG closest to the focal plane. This system (AXAF-OTG-2.0) is offset by 2.50 in (63.5mm) relative to the Grating Nodal system (AXAF-OTG-1.0) of interest for data analysis.

The HETG dispersion direction is rotated 5 deg counterclockwise from Y_A viewed from $X_A = 0$. METG is rotated the same amount clockwise. The inner and outer radii of the OTG are 234.95 and 558.80 mm.

4.1.6 Project FPSI Coordinate System

The Focal Plane Science Instruments coordinate system (X_F, Y_F, Z_F) is essentially identical to the LSI system defined in this document. However, the SE30 [2] definition specifies the origin as the 'desired aim point', while my LSI definition specifically selects a single nominal aim point for each instrument.

4.1.7 SIM and ISIM coordinates

ISIM coordinates are defined in the OBS/SI ICD [1] with their origin at spacecraft coordinates (31.836, 0.0, 0.0) near the focus (and thus defined only while the spacecraft is assembled); SIM coordinates are defined in the System Alignment Plan D17388, with their origin at the SIM/OBA interface. Both are usually measured in inches. I recommend use of the more generally defined data analysis coordinate systems FP (fixed wrt the HRMA) and STF (fixed wrt the SIM) defined below. SIM and OBA coordinates are identical after assembly.

$$(X_{ISIM}, Y_{ISIM}, Z_{ISIM}) = (X_A, Y_A, Z_A) - \begin{pmatrix} 31.836 \\ 0 \\ 0 \end{pmatrix}$$

and

$$(X_{SIM}, Y_{SIM}, Z_{SIM}) = (X_A, Y_A, Z_A) - \begin{pmatrix} 60.336 \\ 0 \\ 0 \end{pmatrix}.$$

4.1.8 SAOSAC coordinates (HRMA-3.0)

The SAOSAC coordinate system $(X_{OSAC}, Y_{OSAC}, Z_{OSAC})$ is slightly different again. In the SAOSAC system, at XRCF, the Z-axis increases towards the SI along the FOA, while the X and Y axes are in the aperture plane with the +Y axis vertical. The origin of SAOSAC coordinates is at ***A1***, which has nodal X-coordinate $X_N(A1) = 872.692$.

$$\begin{pmatrix} X_{OSAC} \\ Y_{OSAC} \\ Z_{OSAC} \end{pmatrix} = \begin{pmatrix} Y_N \\ -Z_N \\ X_N(A1) - X_N \end{pmatrix} \tag{114}$$

4.1.9 Summary of useful HRMA Cartesian systems

$$\begin{pmatrix} X_N \\ Y_N \\ Z_N \end{pmatrix} = \begin{pmatrix} X_H - X_H(H0) \\ Y_H \\ Z_H \end{pmatrix} = \begin{pmatrix} X_N(A1) - Z_{OSAC} \\ +X_{OSAC} \\ -Y_{OSAC} \end{pmatrix} \tag{115}$$

$$= \begin{pmatrix} (SCX - SCX(H0)) * 25.4 \\ SCY * 25.4 \\ SCZ * 25.4 \end{pmatrix}$$

5 Aspect Camera coordinates

(This section is here as a placeholder for now.)

The **Aspect Camera pixel coordinates** (x_{ap}, y_{ap}) run from 0 to 1023 along each axis of the camera. From this array are extracted a set of 4x4 subarrays whose coordinate system, **Aspect subarray coordinates**, consists of a triplet (n_{sa}, x_{sa}, y_{sa}) giving the subarray number and the pixel value (running from 1 to 4 in each axis). Usually, however, we may use the full pixel coordinates when processing the subarrays.

The Aspect Camera CCD is distorted and we will provide a transformation to go from pixel coordinates to **Aspect Camera Tangent Plane coordinates** which represent angles on the sky relative to the camera boresight. Aspect processing will yield an aspect solution which is the transformation of these tangent plane coordinates to **Aspect Camera Sky pixel coordinates** and J2000.0 Sky Coordinates. This solution will then be transferred to the HRMA.

5.1 Fiducial Lights

There are 14 fiducial lights, whose properties are tabulated below. Each fid light is characterized by the angle between the beam centerline and the normal to the STT mounting surface, θ_{tilt}, the

clocking angle in the Y,Z plane (with zero along $+Y$), θ_{clock}, and the half cone angle of the light beam, θ_{zero}. The LSI coordinates of the unit vector along the center of the light beam are

$$\boldsymbol{n}_{LSI} = \begin{pmatrix} \cos\theta_{tilt} \\ \cos\theta_{clock}\sin\theta_{tilt} \\ \sin\theta_{clock}\sin\theta_{tilt} \end{pmatrix}. \tag{116}$$

We also need to know the location of the light in the LSI Y,Z plane. Drawing 301438 [1] shows the positions of the HRC fid lights. For ACIS, it shows the positions of a point A on the fid light which is offset $dA = 9.017$mm from the fid light center; I have corrected the positions to the fid light center by

$$\begin{pmatrix} X_L(Fid) \\ Y_L(Fid) \\ Z_L(Fid) \end{pmatrix} = \begin{pmatrix} X_L(\text{Datum A}) \\ Y_L(\text{Datum A}) \\ Z_L(\text{Datum A}) \end{pmatrix} + dA \begin{pmatrix} 0 \\ -\sin\theta_{clock} \\ \cos\theta_{clock} \end{pmatrix} \tag{117}$$

The tilt, beam width and clocking angles for each light are:

Table 23: Fiducial Light Angles

Name	θ_{tilt} (deg)	θ_{zero} (deg)	θ_{clock} (deg)
ACIS-1	0.45	1.3500	304.37
ACIS-2	0.45	1.3500	237.82
ACIS-3	0.45	1.3500	270.00
ACIS-4	0.60	1.3500	16.12
ACIS-5	0.55	1.3500	161.74
ACIS-6	0.40	1.3500	74.12
HRC-I-1	0.45	1.5833	239.0
HRC-I-2	0.45	1.5833	301.0
HRC-I-3	0.45	1.5833	142.0
HRC-I-4	0.45	1.5833	38.0
HRC-S-1	0.40	1.3833	203.19
HRC-S-2	0.40	1.3833	336.81
HRC-S-3	0.40	1.3833	156.81
HRC-S-4	0.40	1.3833	23.19

The fid light positions and directions in the LSI frames are

Table 24: Fiducial Light Vectors

Name	$(X_{LSI}, Y_{LSI}, Z_{LSI})$	$\boldsymbol{n}_{LSI}$
ACIS-1	(25.40, -43.24, 39.78)	$(0.99997, +0.00443, -0.00648)$

ACIS-2	(25.40, 39.78, 39.78)	$(0.99997, -0.00418, -0.00665)$
ACIS-3	(25.40, 0.00, 46.13)	$(0.99997, +0.00000, -0.00785)$
ACIS-4	(25.40, -102.99, -53.21)	$(0.99995, +0.01006, +0.00291)$
ACIS-5	(25.40, 90.88, -53.43)	$(0.99995, -0.00912, +0.00301)$
ACIS-6	(25.40, -17.42, -84.78)	$(0.99998, +0.00191, +0.00671)$
HRC-I-1	(35.56, 78.49, 130.63)	$(0.99997, -0.00405, -0.00673)$
HRC-I-2	(35.56, -78.49, 130.63)	$(0.99997, +0.00405, -0.00673)$
HRC-I-3	(35.56, 120.09, -93.83)	$(0.99997, -0.00619, +0.00484)$
HRC-I-4	(35.56,-120.09, -93.83)	$(0.99997, +0.00619, +0.00484)$
HRC-S-1	(35.56, 58.37, 25.00)	$(0.99998, -0.00642, -0.00275)$
HRC-S-2	(35.56, -58.37, 25.00)	$(0.99998, +0.00642, -0.00275)$
HRC-S-3	(35.56, 58.37, -25.00)	$(0.99998, -0.00642, +0.00275)$
HRC-S-4	(35.56, -58.37, -25.00)	$(0.99998, +0.00642, +0.00275)$

For ACIS, the ACIS-I LSI frame is used rather than the ACIS-S frame.
For the record, the datum A positions of the ACIS fid lights are:

Table 25: ACIS fid light datums

Light	Y,Z
ACIS-1	$-50.68, +34.69$
ACIS-2	$+32.15, +44.58$
ACIS-3	$-9.02, +46.13$
ACIS-4	$-100.49, -61.87$
ACIS-5	$+93.71, -44.87$
ACIS-6	$-8.75, -87.25$

References

[1] TRW IF1-20, Observatory to Science Instrument ICD, 11 Jan 1996.

[2] TRW SE30, AXAF-I System Alignment Plan, D17388, 11 Jan 1996.

[3] AXAF Transmission Grating Diffraction Coordinates, ASC Memo, D.P. Huenemorder, 2 Apr 1996.

[4] EQ7-002 Rev D.

A Appendix 1: Spherical Coordinate Rotation

A.1 Single axis rotations

Consider unit vectors $\boldsymbol{e_X}$, $\boldsymbol{e_Y}$, $\boldsymbol{e_Z}$ along the axes of a right handed Cartesian system X,Y,Z. Let the operator for a simple anticlockwise rotation of X,Y,Z to X', Y', Z' about a general vector $\boldsymbol{a}$ by angle α be $\mathrm{Rot}_1(\boldsymbol{a}, \alpha)$, so

$$\begin{pmatrix} X' \\ Y' \\ Z' \end{pmatrix} = \mathrm{Rot}_1(\boldsymbol{a}, \alpha) \begin{pmatrix} X \\ Y \\ Z \end{pmatrix}. \tag{118}$$

Further adopt the convention that in a context where a vector is expected, we may simply write X for $\boldsymbol{e_X}$, etc. so that $\mathrm{Rot}_1(-X, \alpha)$ is a rotation around the -X axis. Then

$$\mathrm{Rot}_1(X, \alpha) = \begin{pmatrix} 1 & 0 & 0 \\ 0 & \cos\alpha & \sin\alpha \\ 0 & -\sin\alpha & \cos\alpha \end{pmatrix} \tag{119}$$

$$\mathrm{Rot}_1(Y, \alpha) = \begin{pmatrix} \cos\alpha & 0 & -\sin\alpha \\ 0 & 1 & 0 \\ \sin\alpha & 0 & \cos\alpha \end{pmatrix} \tag{120}$$

$$\mathrm{Rot}_1(Z, \alpha) = \begin{pmatrix} \cos\alpha & \sin\alpha & 0 \\ -\sin\alpha & \cos\alpha & 0 \\ 0 & 0 & 1 \end{pmatrix} \tag{121}$$

A.2 Euler rotations

We define an Euler rotation $\mathrm{Rot}(\phi_E, \theta_E, \psi_E)$ of a Cartesian system X,Y,Z to be the product of three rotations

$$\mathrm{Rot}(\phi_E, \theta_E, \psi_E) = \mathrm{Rot}_1(Z, \psi_E)\mathrm{Rot}_1(Y, \theta_E)\mathrm{Rot}_1(Z, \phi_E) \tag{122}$$

where the rotations apply to the successively rotated axes from right to left in the usual sense of matrix multiplication, giving

$$\mathrm{Rot}(\phi_E, \theta_E, \psi_E) = \begin{pmatrix} \cos\phi_E \cos\theta_E \cos\psi_E - \sin\phi_E \sin\psi_E & \sin\phi_E \cos\theta_E \cos\psi_E + \cos\phi_E \sin\psi_E & -\sin\theta_E \cos\psi_E \\ -\cos\phi_E \cos\theta_E \sin\psi_E - \sin\phi_E \cos\psi_E & -\sin\phi_E \cos\theta_E \sin\psi_E + \cos\phi_E \cos\psi_E & \sin\theta_E \sin\psi_E \\ \cos\phi_E \sin\theta_E & \sin\phi_E \sin\theta_E & \cos\theta_E \end{pmatrix} \tag{123}$$

Note the special cases $\theta_E = 0$ and $\theta_E = \pi$ which give

$$\mathrm{Rot}(\phi_E, 0, \psi_E) = \begin{pmatrix} \cos(\phi_E + \psi_E) & \sin(\phi_E + \psi_E) & 0 \\ -\sin(\phi_E + \psi_E) & \cos(\phi_E + \psi_E) & 0 \\ 0 & 0 & 1 \end{pmatrix} \tag{124}$$

and

$$\mathrm{Rot}(\phi_E, \pi, \psi_E) = \begin{pmatrix} -\cos(\phi_E - \psi_E) & -\sin(\phi_E - \psi_E) & 0 \\ -\sin(\phi_E - \psi_E) & \cos(\phi_E - \psi_E) & 0 \\ 0 & 0 & -1 \end{pmatrix} \tag{125}$$

A.3 Rotations of spherical coordinate systems

Consider a spherical coordinate system (r, θ, ϕ) which is rotated to a new system (r, θ', ϕ'). If we write that an Euler rotation $\mathrm{Rot}(\phi_E, \theta_E, \psi_E)$ is applied, we mean that the Euler rotation defined in the foregoing sections is applied, with the usual spherical to cartesian mapping understood that $\phi = 0$ is along the +X axis and $\theta = 0$ is along the +Z axis. So,

$$r\mathcal{S}(\theta', \phi') = \mathrm{Rot}(\phi_E, \theta_E, \psi_E) r\mathcal{S}(\theta, \phi)$$

We now derive the equations for θ', ϕ' in terms of θ, ϕ and the Euler angles. I'll lay this out in gory detail so that noone else has to do it again.

We compare the Cartesian components explicitly:

$$\begin{pmatrix} \cos\phi' \sin\theta' \\ \sin\phi' \sin\theta' \\ \cos\theta' \end{pmatrix} = \mathrm{Rot}(\phi_E, \theta_E, \psi_E) \begin{pmatrix} \cos\phi \sin\theta \\ \sin\phi \sin\theta \\ \cos\theta \end{pmatrix} \tag{126}$$

$$= \begin{pmatrix} \cos\phi_E \cos\theta_E \cos\psi_E - \sin\phi_E \sin\psi_E & \sin\phi_E \cos\theta_E \cos\psi_E + \cos\phi_E \sin\psi_E & -\sin\theta_E \cos\psi_E \\ -\cos\phi_E \cos\theta_E \sin\psi_E - \sin\phi_E \cos\psi_E & -\sin\phi_E \cos\theta_E \sin\psi_E + \cos\phi_E \cos\psi_E & \sin\theta_E \sin\psi_E \\ \cos\phi_E \sin\theta_E & \sin\phi_E \sin\theta_E & \cos\theta_E \end{pmatrix} \begin{pmatrix} \cos\phi \sin\theta \\ \sin\phi \sin\theta \\ \cos\theta \end{pmatrix}$$

$$= \begin{pmatrix} \cos\phi_E \cos\theta_E \cos\psi_E \cos\phi \sin\theta - \sin\phi_E \sin\psi_E \cos\phi \sin\theta + \sin\phi_E \cos\theta_E \cos\psi_E \sin\phi \sin\theta \\ + \cos\phi_E \sin\psi_E \sin\phi \sin\theta - \sin\theta_E \cos\psi_e \cos\theta \\ \\ -\cos\phi_E \cos\theta_E \sin\psi_E \cos\phi \sin\theta - \sin\phi_E \cos\psi_E \cos\phi \sin\theta - \sin\phi_E \cos\theta_E \sin\psi_E \sin\phi \sin\theta \\ + \cos\phi_E \cos\psi_E \sin\phi \sin\theta + \sin\theta_E \sin\psi_E \cos\theta \\ \\ \cos\phi_E \sin\theta_E \cos\phi \sin\theta + \sin\phi_E \sin\theta_E \sin\phi \sin\theta \\ + \cos\theta_E \cos\theta \end{pmatrix}$$

$$= \begin{pmatrix} \cos\theta_E \cos\psi_E \sin\theta \cos(\phi - \phi_E) + \sin\psi_E \sin\theta \sin(\phi - \phi_E) - \sin\theta_E \cos\psi_E \cos\theta \\ -\cos\theta_E \sin\psi_E \sin\theta \cos(\phi - \phi_E) + \cos\psi_E \sin\theta \sin(\phi - \phi_E) + \sin\theta_E \sin\psi_E \cos\theta \\ \cos\theta_E \cos\theta + \sin\theta_E \sin\theta \cos(\phi - \phi_E) \end{pmatrix}$$

Now we multiply each side by $\mathrm{Rot}_1(Z, -\psi_E)$ giving

$$\begin{pmatrix} \cos\phi' \sin\theta' \cos\psi_E - \sin\phi' \sin\theta' \sin\psi_E \\ \cos\phi' \sin\theta' \sin\psi_E + \sin\phi' \sin\theta' \cos\psi_E \\ \cos\theta' \end{pmatrix} = \begin{pmatrix} \cos\theta_E \cos^2\psi_E \sin\theta \cos(\phi - \phi_E) + \sin\psi_E \cos\psi_E \sin\theta \sin(\phi - \phi_E) - \sin\theta_E \cos^2\psi_E \cos\theta \\ + \cos\theta_E \sin^2\psi_E \sin\theta \cos(\phi - \phi_E) - \cos\psi_E \sin\psi_E \sin\theta \sin(\phi - \phi_E) - \sin\theta_E \sin^2\psi_E \cos\theta \\ \\ \cos\theta_E \sin\psi_E \cos\psi_E \sin\theta \cos(\phi - \phi_E) + \sin^2\psi_E \sin\theta \sin(\phi - \phi_E) - \sin\theta_E \sin\psi_E \cos\psi_E \cos\theta \\ -\cos\theta_E \cos\psi_E \sin\psi_E \sin\theta \cos(\phi - \phi_E) + \cos^2\psi_E \sin\theta \sin(\phi - \phi_E) + \sin\theta_E \cos\psi_E \sin\psi_E \cos\theta \\ \\ \cos\theta_E \cos\theta + \sin\theta_E \sin\theta \cos(\phi - \phi_E) \end{pmatrix} \tag{127}$$

or, collecting up terms,

$$\begin{pmatrix} \sin\theta' \cos(\phi' + \psi_E) \\ \sin\theta' \sin(\phi' + \psi_E) \\ \cos\theta' \end{pmatrix} = \begin{pmatrix} \cos\theta_E \sin\theta \cos(\phi - \phi_E) - \sin\theta_E \cos\theta \\ \sin\theta \sin(\phi - \phi_E) \\ \cos\theta_E \cos\theta + \sin\theta_E \sin\theta \cos(\phi - \phi_E) \end{pmatrix} \tag{128}$$

giving the results

$$\boxed{\begin{aligned} \theta' &= \cos^{-1}\left(\cos\theta_E \cos\theta + \sin\theta_E \sin\theta \cos(\phi - \phi_E)\right) \\ \phi' &= \arg\left(\cos\theta_E \sin\theta \cos(\phi - \phi_E) - \sin\theta_E \cos\theta, \sin\theta \sin(\phi - \phi_E)\right) - \psi_E \end{aligned}} \tag{129}$$

An alternative way to construct the rotation matrix is by constructing the unit axis triad of the new system. We describe the transformation by providing the coordinates (θ_0, ϕ_0) of the new pole in the old system, and the 'roll angle' γ of the new X-axis relative to the old one. The old axes are

$$\boldsymbol{e}_X = (1,0,0), \boldsymbol{e}_Y = (0,1,0), \boldsymbol{e}_Z = (0,0,1). \tag{130}$$

Then

$$\boldsymbol{e}'_Z = \mathcal{S}(\theta_0, \phi_0) \tag{131}$$

and

$$\boldsymbol{e}_E = \boldsymbol{e}_Z \wedge \boldsymbol{e}'_Z \tag{132}$$

giving a vector in the old and new equatorial planes pointing 'east'. Then

$$\boldsymbol{e}_N = \boldsymbol{e}'_Z \wedge \boldsymbol{e}_E. \tag{133}$$

Now we roll the tangent plane,

$$\boldsymbol{e}'_X = \cos\gamma \boldsymbol{e}_E - \sin\gamma \boldsymbol{e}_N \tag{134}$$

and

$$\boldsymbol{e}'_Y = \sin\gamma \boldsymbol{e}_E + \cos\gamma \boldsymbol{e}_N. \tag{135}$$

The components of the three new axis vectors in the old system make up the elements of the rotation matrix,

$$\mathrm{Rot}(\pi/2 + \gamma, \theta_0, \pi - \phi_0) = \left(\begin{array}{ccc} \boldsymbol{e}'_X & \boldsymbol{e}'_Y & \boldsymbol{e}'_Z \end{array} \right). \tag{136}$$

The Euler angles can be found from the axis vectors as follows:

$$\begin{array}{ll} \theta_E & = \cos^{-1} \boldsymbol{e}'_Z.\boldsymbol{e}_Z \\ \phi_E & = \arg\left(\boldsymbol{e}'_X.\boldsymbol{e}_Z/\sin\theta_E, \boldsymbol{e}'_Y.\boldsymbol{e}_Z/\sin\theta_E\right) \quad ll \\ \psi_E & = \arg\left(-\boldsymbol{e}'_Z.\boldsymbol{e}_X/\sin\theta_E, \boldsymbol{e}'_Z.\boldsymbol{e}_Y/\sin\theta_E\right) \end{array} \tag{137}$$

A.4 Euler rotation angles for axis relabelling

Here I tabulate the Euler angles which describe the simple cases of relabelling of the X, Y, Z axes such as $(X', Y', Z') = (Y, -Z, -X)$. We have

$$\left(\begin{array}{c} X' \\ Y' \\ Z' \end{array} \right) = \mathrm{Rot}(\phi_E, \theta_E, \psi_E) \left(\begin{array}{c} X \\ Y \\ Z \end{array} \right)$$

and the inverse

$$\left(\begin{array}{c} X \\ Y \\ Z \end{array} \right) = \mathrm{Rot}(\phi'_E, \theta'_E, \psi'_E) \left(\begin{array}{c} X' \\ Y' \\ Z' \end{array} \right)$$

Table 26: Euler angles for axis relabelling

(X', Y', Z')	ϕ_E	θ_E	ψ_E	ϕ'_E	θ'_E	ψ'_E
$+X, +Y, +Z$	0	0	0	0	0	0
$+X, -Y, -Z$	0	180	0	0	180	0
$+Y, -X, +Z$	90	0	0	270	0	0
$+Y, +X, -Z$	90	180	0	180	180	90
$-X, -Y, +Z$	180	0	0	180	0	0
$-X, +Y, -Z$	180	180	0	180	180	0
$-Y, +X, +Z$	270	0	0	90	0	0
$-Y, -X, -Z$	270	180	0	270	180	0
$-Z, +Y, +X$	0	90	0	180	90	180
$+Y, +Z, +X$	0	90	90	90	90	180
$+Z, -Y, +X$	0	90	180	0	90	180
$-Y, -Z, +X$	0	90	270	270	90	180
$-Z, -X, +Y$	90	90	0	180	90	90
$-X, +Z, +Y$	90	90	90	90	90	90
$+Z, +X, +Y$	90	90	180	0	90	90
$+X, -Z, +Y$	90	90	270	270	90	90
$-Z, -Y, -X$	180	90	0	180	90	0
$-Y, +Z, -X$	180	90	90	90	90	0
$+Z, +Y, -X$	180	90	180	0	90	0
$+Y, -Z, -X$	180	90	270	270	90	0
$-Z, +X, -Y$	270	90	0	180	90	270
$+X, +Z, -Y$	270	90	90	90	90	270
$+Z, -X, -Y$	270	90	180	0	90	270
$-X, -Z, -Y$	270	90	270	270	90	270

A.5 WCS Convention

When we deal with celestial coordinates we usually use a latitude-longitude system. In the WCS paper, Griesen and Calabretta describe a rotation to celestial coordinates (α, δ) from a native longitude and latitude (ϕ_w, θ_w) (where the subscripts are added by me to distinguish them from the variables already introduced).

In terms of the standard spherical polar variables used above,

$$\phi_w = \phi, \quad \theta_w = \pi/2 - \theta$$

and

$$\alpha = \phi', \delta = \pi/2 - \theta'.$$

They also use the new coordinates of the north pole of the old system (α_P, δ_P) and the longitude in the old system ϕ_P of the new system's north pole to describe the parameters of the rotation. In terms of our Euler angles,

$$\begin{aligned} \alpha_P &= \pi - \psi_E \\ \delta_P &= \pi/2 - \theta_E \\ \phi_P &= \phi_E \end{aligned} \tag{138}$$

Their standard rotation is then

$$r\mathcal{S}(\pi/2 - \delta, \alpha) = \mathrm{Rot}(\phi_P, \pi/2 - \delta_P, \pi - \alpha_P) r\mathcal{S}(\pi/2 - \theta_w, \phi_w)$$

in our notation.

Equation 129 becomes

$$\delta = \sin^{-1}\left(\sin\theta_w \sin\delta_P + \cos\theta_w \cos\delta_P \cos(\phi_w - \phi_P)\right) \tag{139}$$

and

$$\alpha = \arg\left(\sin\delta_P \cos\theta_w \cos(\phi_w - \phi_P) - \cos\delta_P \sin\theta_w, \cos\theta_w \sin(\phi_w - \phi_P)\right) - \pi + \alpha_P. \tag{140}$$

Note that in terms of the roll angle,

$$\phi_P = \pi + \gamma \tag{141}$$

so

$$r\mathcal{S}(\pi/2 - \delta, \alpha) = \mathrm{Rot}(\pi + \gamma, \pi/2 - \delta_P, \pi - \alpha_P) r\mathcal{S}(\pi/2 - \theta_w, \phi_w)$$

Now let's consider the conversion from tangent plane to sky pixel coordinates. At a given time we have an instantaneous aspect solution $(\alpha_A, \delta_A, \gamma_A)$ in which the transformation to RA and Dec is given by

$$r\mathcal{S}(\pi/2 - \delta, \alpha) = \mathrm{Rot}(\pi + \gamma_A, \pi/2 - \delta_A, \pi - \alpha_A) \begin{pmatrix} X_{PTP} \\ Y_{PTP} \\ Z_{PTP} \end{pmatrix}$$

We wish to transform this to PSP coordinates in which the center of the field is at the nominal location α_P, δ_P. To go from PSP coordinates to RA and Dec one has simply

$$r\mathcal{S}(\pi/2 - \delta, \alpha) = \mathrm{Rot}(\pi, \pi/2 - \delta_P, \pi - \alpha_P) \begin{pmatrix} X_{PSP} \\ Y_{PSP} \\ Z_{PSP} \end{pmatrix}.$$

Hence

$$\begin{pmatrix} X_{PSP} \\ Y_{PSP} \\ Z_{PSP} \end{pmatrix} = \mathrm{Rot}(\pi - \alpha_P, \pi/2 - \delta_P, \pi)\mathrm{Rot}(\pi + \gamma_A, \pi/2 - \delta_A, \pi - \alpha_A) \begin{pmatrix} X_{PTP} \\ Y_{PTP} \\ Z_{PTP} \end{pmatrix}$$

A.6 Jonathan's Angular Convention

To describe angular coordinate systems fully and concisely, I introduce a new convention which summarizes the different ways Cartesian coordinates map to an angle. This convention is applied both to the polar and azimuthal angles (θ', ϕ') of a 3D system and uses as reference the 'standard' spherical polar convention that the azimuthal angle ϕ is $\arg(X, Y)$, i.e. increasing from 0 to 360 counterclockwise in the X Y plane starting from the X axis, and that the polar angle θ is $\arg(Z, XY)$, i.e. increasing from 0 to 180 (or in some applications 360) from the Z-axis north pole towards the equator. In contrast, in everyday life we often use the latitude/longitude system in which the azimuthal angle is measured from -180 to $+180$ and the polar angle runs from $+90$ at the north pole to -90 at the south pole. There are a number of other cases which are useful - for instance the 'clock face' convention where the angle is measured from the +Y axis (noon) through the +X axis (3 o'clock).

We can compactly describe all of these with three digits $r = 0, 1, 2, 3$ (rotated), $e = 0, 1$ (east-west), and $c = 0, 1$ (clockwise) follows:

$$\theta' = A_{rec}(\theta) = A_{0e0}\left((-1)^c\left(\theta - r\pi/2\right)\right) \tag{142}$$

where

$$A_{0e0}(\theta) = \begin{cases} \theta + 2\pi & (-2\pi \le \theta < -\pi) \\ \theta + 2\pi(1-e) & (-\pi \le \theta < 0) \\ \theta & (0 \le \theta < \pi) \\ \theta - 2\pi e & (\pi \le \theta < 2\pi) \end{cases} \tag{143}$$

where θ is the standard convention angle in radians and θ' is the transformed angle in radians. The offset by r rotates the origin by 90 degrees, the c factor reverses the handedness of the coordinates, and the e factor as implemented by the A_{0e0} function forces the angle to lie between -180 and 180 if $e = 1$ or between 0 and 360 if $e = 0$.

The inverse is

$$\theta = A^{-1}_{rec}(\theta') = \mathrm{mod}(r\pi/2 + (-1)^c\theta', 2\pi) \tag{144}$$

I also specify that saying that μ, λ is a spherical system using convention $(r_1e_1c_1, r_2e_2c_2)$ means a spherical polar coordinate system with the polar angle described using convention $r_1e_1c_1$ and the azimuthal angle using convention $r_2e_2c_2$ (in other words, I stipulate that you always put the polar angle first). Thus

$$\mu = A_{r_1e_1c_1}(\theta), \quad \lambda = A_{r_2e_2c_2}(\phi). \tag{145}$$

Further I define the following standard names for the different possible choices, and note the inverse functions:

Table 27: Angular convention summary

r, e, c	Name	$(\cos\theta, \sin\theta)$
000	Standard	$(\cos\theta', \sin\theta')$
001	Lefthand	$(\cos\theta', -\sin\theta')$
010	East-West	$(\cos\theta', \sin\theta')$
011	West-East	$(\cos\theta', -\sin\theta')$
100	Rotated	$(-\sin\theta', \cos\theta')$
101	Clock	$(\sin\theta', \cos\theta')$
110	Rotated E-W	$(-\sin\theta', \cos\theta')$
111	Latitude	$(\sin\theta', \cos\theta')$

For example, suppose we say that (X,Y,Z) is a Cartesian system, and (r, θ, ϕ) is its standard native spherical system (000, 000). Then define a new system (r, μ, λ) to be a Latitude, East-West system or (111, 010). This tells us that (in degrees):

$$\begin{aligned} \mu &= A_{111}(\theta) \quad = A_{010}(90-\theta) \quad = \begin{cases} 90-\theta & (0 \le \theta < 270) \\ 450-\theta & (270 \le \theta < 360) \end{cases} \\ \lambda &= A_{010}(\phi) \qquad\qquad\qquad\quad = \begin{cases} \phi & (0 \le \phi < 180) \\ \phi - 360 & (180 \le \phi < 360) \end{cases} \end{aligned} \tag{146}$$

so

$$\lambda = arg_1(X, Y); \mu = \sin^{-1}(Z/r) \tag{147}$$

where $\arg_1$ is defined to run from $-\pi$ to $+\pi$, and

$$\begin{pmatrix} X \\ Y \\ Z \end{pmatrix} = \begin{pmatrix} r\cos\phi\sin\theta \\ r\sin\phi\sin\theta \\ r\cos\theta \end{pmatrix} = \begin{pmatrix} r\cos A_{010}^{-1}(\lambda)\sin A_{111}^{-1}(\mu) \\ r\sin A_{010}^{-1}(\lambda)\sin A_{111}^{-1}(\mu) \\ r\cos A_{111}^{-1}(\mu) \end{pmatrix} \tag{148}$$

Having such a convention is particularly useful in a generic coordinate conversion program; it lets us tell software in a generic way what the relationship between a spherical and a cartesian system is.

For the spherical systems defined in this document, the conventions are:

Table 28: Angular meta-convention for AXAF spherical coordinates

AXAF-HSC-1.1	(000,001)	Off-axis angle (standard), Azimuth (Lefthand)
AXAF-HSC-1.2	(000,000)	Standard
AXAF-HSC-2.1	(111,000)	Azimuth (latitude), elevation (standard)
AXAF-HSC-3.0	(111,010)	Yaw (latitude), Pitch (East-West)

B Appendix B: Pixel systems and WCS convention

B.1 Physical and pixel systems

In general, each pixel coordinate system $(XPIX, YPIX)$ has a corresponding linear physical system (X_p, Y_p, Z_p) related by

$$\begin{aligned} X_p - X_{p0} &= s_x(XPIX - XPIX0) * \Delta \\ Y_p - Y_{p0} &= s_y(YPIX - YPIX0) * \Delta \end{aligned} \tag{149}$$

where s_x and s_y are each $+1$ or -1 to determine the handedness of the physical system with respect to the pixel system, and Δ is the pixel size in physical units per pixel. (XPIX0, YPIX0) is the Reference Pixel and (X_{p0}, Y_{p0}) is the Reference Physical Coordinate. The Z_p coordinate is defined to be zero in the pixel plane and to complete a right handed set with X_p, Y_p.

We can attach a physical system to a pixel system in a data file using the World Coordinate System keywords. For a 2D image with XPIX on axis 1 and YPIX on axis 2,

Table 29: WCS Keywords

WCS Keyword	Value
CTYPE1	Name of X_p
CTYPE2	Name of Y_p
CDELT1	$s_x\Delta$
CDELT2	$s_y\Delta$
CRPIX1	XPIX0
CRPIX2	YPIX0
CRVAL1	X_{p0}
CRVAL2	Y_{p0}

We can also attach an angular system for tangent plane coordinates (to be added later).

Here are the parameters of the pixel to physical conversions for the systems defined in earlier sections.

Table 30: Physical to pixel conversion parameters

Pixel system	Physical System	XPIX0, YPIX0	X_{p0}, Y_{p0}	Δ	s_x, s_y
CHIP	CPC	0.5, 0.5	0.0, 0.0	Δ_p	$+1, +1$
TP	PTP	TPX0, TPY0	0.0, 0.0	Δ_s	$-1, +1$
SKY	PSP	TPX0, TPY0	0.0, 0.0	Δ_s	$-1, +1$

C Appendix C: HRC MCP corner positions in LSI coordinates

Table 31: HRC MCP corner positions in LSI coordinates

Chip	CPC coords for MCP	HRC-I,S LSI coords	
HRC-I	LL	(2.672 , 2.672 , 0.000)	(0.000 , 0.000 , 70.711)
HRC-I	LR	(102.672 , 2.672 , 0.000)	(0.000 , 70.711 , 0.000)
HRC-I	UR	(102.672 , 102.672 , 0.000)	(0.000 , 0.000 , -70.711)
HRC-I	UL	(2.672 , 102.672 , 0.000)	(0.000 , -70.711 , 0.000)
HRC-S1	LL	(-0.332 , 6.111 , 0.000)	(2.489 , 155.875 , -13.500)
HRC-S1	LR	(26.668 , 6.111 , 0.000)	(2.489 , 155.875 , 13.500)
HRC-S1	UR	(26.668 , 106.111 , 0.000)	(0.000 , 55.905 , 13.500)
HRC-S1	UL	(-0.332 , 106.111 , 0.000)	(0.000 , 55.905 , -13.500)
HRC-S2	LL	(-0.332 , 2.672 , 0.000)	(0.000 , 54.000 , -13.500)
HRC-S2	LR	(26.668 , 2.672 , 0.000)	(0.000 , 54.000 , 13.500)
HRC-S2	UR	(26.668 , 102.672 , 0.000)	(0.000 , -45.999 , 13.500)
HRC-S2	UL	(-0.332 , 102.672 , 0.000)	(0.000 , -45.999 , -13.500)
HRC-S3	LL	(-0.332 , -0.767 , 0.000)	(0.000 , -47.904 , -13.500)
HRC-S3	LR	(26.668 , -0.767 , 0.000)	(0.000 , -47.904 , 13.500)
HRC-S3	UR	(26.668 , 99.233 , 0.000)	(2.134 , -147.881 , 13.500)
HRC-S3	UL	(-0.332 , 99.233 , 0.000)	(2.134 , -147.881 , -13.500)

D Appendix D: FAM encoders and FAM feet

D.1 The FAM

The center of the FAM aperture (FAM payload interface plane) is located at FA0(DFC) = (30.5 in, 0, 0), or (if there is no misalignment) FA0(XRCF) = $(-f + 30.5in, 0, 0)$.

The moving FAM frame, FAM coordinates, is related to the LSI frame by R(LSI,FAM) = R(XRCF,DFC). We have

$$P(FAM) = R(DFC, FAM)(P(DFC) - FR(DFC)) \tag{150}$$

where FR is the position of the actual FAM relative to its default position. We also have

$$P(LSI) = R(X, LSI)(P(X) - S(X)) \tag{151}$$

where S is the position of the SIM and X is the XRCF frame translated to an origin at S0. In our notation, eq.7 of SER is

$P(DFC) - FR(DFC) \;\; = \;\; R(FAM, DFC)P(FAM)$

$$
\begin{aligned}
&= R(FAM,DFC)R(LSI,FAM)P(LSI) \\
&= R(FAM,DFC)R(LSI,FAM)R(X,LSI)(P(X)-S(X)) \\
&= R(FAM,DFC)R(X,DFC)R(X,LSI)\left(R(DFC,X)P(DFC)-S(X)\right)
\end{aligned}
\tag{152}
$$

In particular, taking P(DFC)=0 (origin of DFC coords),

$$FR(DFC) = R(FAM,DFC)R(X,DFC)R(X,LSI)S(X) \tag{153}$$

and so

$$P(DFC) = R(FAM,DFC)R(X,DFC)R(X,LSI)(R(DFC,X)P(DFC)) \tag{154}$$

for all P, hence

$$R(DFC,FAM) = R(XRCF,DFC)R(XRCF,LSI)R(DFC,XRCF) \tag{155}$$

or

$$R(FAM,DFC) = R(X,DFC)R(LSI,X)R(DFC,X) \tag{156}$$

giving

$$FR(DFC) = R(XRCF,DFC)(S(XRCF)-S0(XRCF)) = S(DFC). \tag{157}$$

The quantities R(DFC,FAM) and FR(DFC) define the rotation and translation of the FAM needed in terms of the required SIM displacements S(XRCF) and R(XRCF,LSI).

D.2 Movement of the FAM feet

The three feet of the FAM are called A, B and C but I'll number them as foot λ, λ = A,B,C. Each foot can move in three (non-orthogonal) displacement directions $\boldsymbol{T}_i^\lambda$ fixed in the DFC frame. We write the components of these vectors in the DFC frame as $\boldsymbol{T}_{ij}^\lambda$.

The matrix of vectors $\boldsymbol{T}_{ij}^\lambda$ is

$$
\begin{array}{l}\boldsymbol{T}^A \\ \boldsymbol{T}^B \\ \boldsymbol{T}^C\end{array} = \begin{pmatrix} (1,TAy_x,TAz_x) & (TAx_y,1,TAz_y) & (TAx_z,TAy_z,1) \\ (1,TBy_x,TBz_x) & (0,1,0) & (TBx_z,TBy_z,1) \\ (1,0,0) & (0,1,0) & (TCx_z,TCy_z,1) \end{pmatrix} \tag{158}
$$

where the zeros come from redundancies in the directions. Approximately, $\boldsymbol{T}_{ij}^\lambda = \delta_{ij}$ i.e. the T vectors lie along the DFC unit axis vectors. Thus for instance

$$\boldsymbol{T}_{\boldsymbol{1}}^{\boldsymbol{A}}(DFC) \sim (1,0,0). \tag{159}$$

Let the origin (boresight) positions of the FAM feet be $\boldsymbol{O_{FF}}^\lambda$. The DFC coordinates of a general point with FAM coordinates P(FAM) are

$$P(DFC) = R(FAM,DFC)P(FAM) + FR(DFC). \tag{160}$$

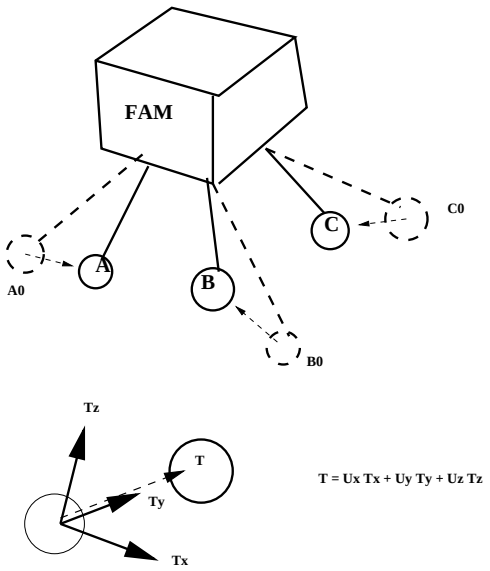

Figure 23: FAM Feet

The FAM coordinates of each foot $P^{\lambda}_{FF}(FAM)$ remain constant during motion of the FAM, since the feet are rigid with respect to the FAM; thus the FAM coordinates of the feet are numerically equal to the DFC coordinates at the origin position, i.e.

$$\boldsymbol{P_{FF}}^{\lambda}(FAM) = \boldsymbol{O_{FF}}^{\lambda}(DFC) \tag{161}$$

and so its DFC coordinates are

$$\boldsymbol{P_{FF}}^{\lambda}(DFC) = R(FAM, DFC)\boldsymbol{O_{FF}}^{\lambda}(DFC) + \boldsymbol{FR}(DFC) \tag{162}$$

and hence the foot has been displaced by

$$\boldsymbol{\Delta F}^{\lambda} = (R(FAM, DFC) - 1)\boldsymbol{O_{FF}}^{\lambda} + \boldsymbol{FR} \tag{163}$$

Let the motor displacement along foot *lambda*, displacement direction j be U^{λ}_{j}. Then the components of the displacement in DFC coordinates are

$$\Delta F^{\lambda}_{i} = U^{\lambda}_{j} T^{\lambda}_{ij} \tag{164}$$

(where the summation convention does not apply to the λ index) so

$$U^{\lambda}_{j} T^{\lambda}_{ij} = (R_{ij}(FAM, DFC) - \delta_{ij})O^{\lambda}_{j} + FR_{i} \tag{165}$$

or

$$U_k^\lambda = (T^{-1})_k^\lambda i \left((R_{ij}(FAM, DFC) - \delta_{ij}) O_j^\lambda + FR_i \right) \tag{166}$$

We now use the relation

$$R(FAM, DFC) = R(XRCF, DFC) R(LSI, XRCF) R(DFC, XRCF) = R^{XD} R^{LX} R^{DX} \tag{167}$$

where we introduce in the second form a more compact notation; then:

$$U_k^\lambda = (T^{-1})_k^\lambda i \left((R_{im}^{XD} R_{mn}^{LX} R_{nj}^{DX} - \delta_{ij}) O_j^\lambda + FR_i \right) \tag{168}$$

This equation allows us to derive the required motor displacements for a given XRCF configuration (R_{ij}^{LX}, FR_i). We can also invert it to find the actual XRCF configuration given the encoder values.

First we relabel the six independent motor axis values as integers g(λ, i)=1,6 as follows:

$$\begin{array}{rcl} g(A,1) & = & 1 \\ g(A,2) & = & 2 \\ g(A,3) & = & 3 \\ g(B,1) & = & 4 \\ g(B,3) & = & 5 \\ g(C,3) & = & 6 \end{array} \tag{169}$$

and ignore other combinations of $lambda, i$. We similarly introduce the six independent XRCF configuration parameters roll, pitch, yaw, FR1, FR2, FR3. Now we have six equations in six unknowns. Let's write the R^{LX} matrix in terms of the nominal configuration value and the small change from the nominal configuration. Then

$$R^{LX} = R_N^{LX} + dR_y \Delta\alpha_y + dR_z \Delta\alpha_z + dR_\psi \Delta\psi \tag{170}$$

where

$$dR_y = \begin{pmatrix} -\sin\alpha_z \cos\alpha_y & \cos\alpha_z \cos\alpha_y \cos r & -\cos\alpha_z \cos\alpha_y \sin r \\ -\cos\alpha_z & -\sin\alpha_z \cos r & \sin\alpha_z \sin r \\ -\sin\alpha_z \sin\alpha_y & \cos\alpha_z \sin\alpha_y \cos r & -\cos\alpha_z \sin\alpha_y \sin r \end{pmatrix} \tag{171}$$

$$dR_z = \begin{pmatrix} -\cos\alpha_z \sin\alpha_y & -\sin\alpha_z \sin\alpha_y \cos r - \cos\alpha_y \sin r & \sin\alpha_z \sin\alpha_y \sin r - \cos\alpha_y \cos r \\ 0 & 0 & 0 \\ \cos\alpha_z \cos\alpha_y & \sin\alpha_z \cos\alpha_y \cos r - \sin\alpha_y \sin r & -\sin\alpha_y \cos r \end{pmatrix} \tag{172}$$

$$dR_\psi = \begin{pmatrix} 0 & -\sin\alpha_z \cos\alpha_y \sin r - \sin\alpha_y \cos r & -\sin\alpha_z \cos\alpha_y \cos r + \sin\alpha_y \cos r + \sin\alpha_y \sin r \\ 0 & -\cos\alpha_z \sin r & -\cos\alpha_z \cos r \\ 0 & -\sin\alpha_z \sin\alpha_y \sin r + \cos\alpha_y \cos r & -\cos\alpha_y \sin r \end{pmatrix} \tag{173}$$

Further assuming the DFC to XRCF boresight angles to be small we write

$$R^{XD} = \begin{pmatrix} 1 & \phi_{EF} & -\theta_{EF} \\ -\phi_{EF} & 1 & \psi_{EF} \\ \theta_{EF} & -\psi_{EF} & 1 \end{pmatrix} \tag{174}$$

and so

$$R^{XD} dR^{LX} R^{DX} = \begin{pmatrix} dR11 + \phi(dR21 + dR12) - \theta(dR31 + dR13) & dR12 + \phi(dR22 - dR11) - \theta dR32 + \psi dR13 & dR13 + \phi dR23 + \theta(dR11 \\ dR21 + \phi(dR22 - dR11) + \psi dR31 - \theta dR23 & dR22 - \phi(dR21 + dR12) + \psi(dR23 + dR32) & dR23 - \phi dR13 + \psi(dR3 \\ dR31 + \theta(dR11 - dR33) - \psi dR21 + \phi dR32 & dR32 + \theta dR12 + \psi(dR33 - dR22) - \phi dR31 & dR33 + \theta(dR31 + dR13) \end{pmatrix} \tag{175}$$

D.3 Dither correction

We need the LSI origin as a function of time. Then we can convert to HRMA source coordinates.

We get six translation stage encoders, measuring $U1_1(UAx)$, $U1_2(UAy)$, $U1_3(UAz)$, $U2_1(UBx)$, $U2_3(UBz)$, $U3_3(UCz)$. From these we can derive the DFC positions of the FAM feet. We need to invert to get the FAM parameters FR(DFC) and R(DFC,FAM). The formula

$$FF_i(DFC) = R(FAM, DFC)FF0_i(DFC) + FR(DFC) \tag{176}$$

represents 9 simultaneous equations in six unknowns (3 Euler angles and 3 FR coordinates).

1. **Encoders to FAM foot positions**:

$$FF_i(DFC) = FF0_i(DFC) + U(i)_j \boldsymbol{T}_{ij} \tag{177}$$

2. **FAM foot positions to FAM position and orientation:** Calculate R(DFC,FAM) and FR(DFC) by inverting the equation for FF_i.

3. **SI frame position and orientation from FAM:**

   The SI origin is at

$$S(XRCF) = S0(XRCF) + R(DFC, XRCF)FR(DFC) \tag{178}$$

   and the orientation is

$$R(LSI, XRCF) = R(DFC, XRCF)R(DFC, FAM)R(XRFC, DFC) \tag{179}$$

   We derive the offsets from nominal, i.e. ΔS, $\Delta\alpha_y$, $\Delta\alpha_z$, and hence get the correction factors from DETX, DETY to X, Y in the form of an aspect solution.

E Appendix E: Note on existing aspect solution software

For the record, here is the formula for applying aspect as implemented in the PROS system: given nominal roll θ, detector pixel center $X0, Y0$ and aspect translation offsets A_x, A_y and roll offset A_r we have

$$\begin{aligned}(X - X0) &= (DETX - X0)\cos(\theta + A_r) - (DETY - Y0)\sin(\theta + A_r) + A_x\cos\theta - A_y\sin\theta \\ (Y - Y0) &= (DETX - X0)\sin(\theta + A_r) + (DETY - Y0)\cos(\theta + A_r) + A_x\sin\theta + A_y\cos\theta\end{aligned} \tag{180}$$